SAND76-0653
NUREG766518
Unlimited Release

NRC-7

Annular Core Pulse Reactor Upgrade Quarterly Report July - September 1976

Reactor Research and Development Department

Prepared by Sandia Laboratories, Albuquerque,
New Mexico 87115 and Livermore, California 94500
for the United States Nuclear Regulatory Commission
under ERDA Contract AT(29-1)-789.

Printed January 1977

Sandia Laboratories
Nuclear Fuel Cycle Programs

Issued by Sandia Laboratories, operated for the United States
Energy Research & Development Administration by Sandia Corporation.

DISCLAIMER

SAND76-0653
NUREG766518
Unlimited Release
Printed January 1977

NRC-7

ANNULAR CORE PULSE REACTOR UPGRADE QUARTERLY REPORT*
July - September 1976

Submitted by
Reactor Research and Development Department
Sandia Laboratories, Albuquerque, New Mexico 87115

Approved: _____
Manager, Reactor Research and Development

_____
Director, Nuclear Fuel Cycle Programs

*This work was supported by the U.S. Nuclear Regulatory Commission Project No. A1032 and the U.S. Energy Research and Development Administration Under Contract AT(29-1)-789.

CONTENTS

	Page
INTRODUCTION	
Task 1. Safety, Documentation, and Compliance	6
Task 2. Core Nuclear Design	6
Task 3. Console Development	6
Task 4. Mechanical Design	6
Task 5. Fuel Element Design	6
Task 6. Primary Fuel Material Studies	6
Task 7. Secondary Fuel Material Studies	7
Task 8. Driver Core Fuel Element	7
Task 9. Diagnostic System	7
Project Schedule	7
CHAPTER I. Task 1. Safety, Compliance, and Documentation	9
Introduction	9
Safety Analysis Report (SAR)	9
Accident Analysis	9
Quality Assurance Program	10
CHAPTER II. Task 2. Core Nuclear Design	11
CHAPTER III. Task 3. Console Development	18
CHAPTER IV. Task 4. Mechanical Design	19
Cooling System	19
Auxiliary Hoist	19
Ventilation System	19
CHAPTER V. Task 5. Fuel Element Design	21
Introduction	21
Heat Transfer Calculations	21
Element Section Test	29
CHAPTER VI. Task 6. UO_2-BeO Fuel Development (Primary Fuel Studies)	34
Pulse Testing	34
Results of Testing	35
Element Section Test	36
Compatibility Studies	41
CHAPTER VII. Task 7. Secondary Fuel Fuel Material Studies	44
Introduction	44
Reactor Pulse Test Results	47
Thermophysical Properties	47
Mechanical Properties	47
Discussion	52
CHAPTER VIII. Task 8. Driver Core Fuel Element	53
Introduction	53
In-Pile Tests	53
CHAPTER IX. Task 9. Diagnostic System	54

ILLUSTRATIONS

Figure		Page
1	ACPR Upgrade Schedule	8
2	Reactivity Loss Curves for ACPR and UC-ZrC-C Upgrade	13
3	Comparison of Pulse Shape for Current ACPR and UC-ZrC-C Upgrade	14
4	Performance Temperature Criticality Curves for Graphite-Hydride Two-Region Core	16
5	Be-UO_2 Fuel Element Design	22
6	(UC-ZrC)-Graphite Fuel Element Design	24
7	Steady State Operation - Maximum Fuel Temperature versus Element Power and Gap Size	26
8	Peak Clad Heat Flux for Steady State and Pulse Operation	27
9	(UC-ZrC)-Graphite Fuel Element Clad Temperature versus Element Power	28
10	Effect of (UC-ZrC)-C Thermal Conductivity on Peak Steady State Fuel Temperature	30
11	Element Section Test Apparatus	31
12	(UC-ZrC)-C Element Section Test Results	32
13	Stacked Niobium Cups with Fuel	37
14	Series 1, Test #5 -- 700 ml Demineralized Water; 50 percent Maximum Pulse; 0.5 inch Polyethylene	39
15	Series 1, Test #7 -- 700 ml Demineralized Water; 50 percent Maximum Pulse, 0.75 inch Polyethylene	40
16	SEM of As-Received Hot Pressed BeO-UO_2 Sample	42
17	Niobium Map of Figure 16	42
18	SEM of Heat Treated BeO-UO_2 Sample	43
19	Niobium Map of Figure 18	43
20	Photomicrographs of Graphite-Based Fuel Fabrication and Characterization Studies	46

TABLES

Table		
I	Comparison of Measured and Calculated Kinetic Parameters	15
II	Basic Characteristics of UC-ZrC-C Reference Core	17
III	Design Concept for BeO-UO_2 Fuel Element	23
IV	Design Concept for (UC-ZrC)-Graphite Fuel Element	23
V	BeO-UO_2 Fuel Test Cold Pressed and Sintered 1/4-High Dual Slotted Outer Annuli	34
VI	Fuel Element Section Test Results	38
VII	Energy Deposition as a Function of Axial Position	38
VIII	Fabricated and Characterized Graphite-Based Fuels	45
IX	Thermal Expansion	48
X	Thermal Diffusivity	48
XI	Mechanical Properties of Lot No. SL017	49
XII	Mechanical Properties of Lot No. SL018	50
XIII	Mechanical Properties of Lot No. SL019	51

ANNULAR CORE PULSE REACTOR UPGRADE QUARTERLY REPORT

INTRODUCTION

The progress on the ACPR Upgrade during FY75 is described in References 1, 2, and 3. Beginning with FY76, the ACPR Upgrade progress is reported in quarterly reports separate from reports on the Fast Reactor Safety Research Program.[4-6]

Funding for the ACPR Upgrade is being provided jointly by NRC/DRSR and ERDA/DMA, since the improved reactor will be beneficial to the programs of both agencies.

The object of the ACPR Upgrade is to arrive at a reactor modification which will provide an increased pulsed neutron fluence in the irradiation cavity without an increased degradation of the pulse duration. The upgraded reactor will also have an increased steady-state neutron flux. The approach to the upgrade modification involves a two-region core concept. The inner region, surrounding the irradiation cavity, consists of a high-heat-capacity fuel which will sustain a large fission energy deposition. The outer region consists of a uranium-zirconium hydride fuel similar to the present ACPR fuel. This reactor modification will make use of the majority of the existing reactor structure and can be accomplished in a relatively short time.

The ACPR Upgrade project is divided into nine tasks to improve management of the overall project and to maintain close control of the project budget. This report discusses the progress on each task in a separate chapter. The individual tasks and a brief description of each are given below.

Task 1. Safety, Documentation, and Compliance (J. A. Reuscher, Supervisor)

This task involves the preparation of the safety analysis report and the technical specifications for the upgraded reactor. These documents must be submitted to ERDA Division of Safety, Standards and Compliance for review and approval prior to startup of the reactor. Compliance with the requirements contained in 10CFR50 is a part of this task; these include an independent design review and quality assurance program. In addition, the initial test planning for the reactor is a part of this task.

Task 2. Core Nuclear Design (J. A. Reuscher, Supervisor)

This task includes core neutron physics studies, determination of control rod configurations, and the prediction of experimental conditions. Correlation of calculational techniques with the present ACPR is included.

Task 3. Console Development (J. E. Powell, Supervisor)

This task is concerned with the design, development, and procurement of a control system which follows IEEE 279 standards.

Task 4. Mechanical Design (J. H. Davis, Supervisor)

Mechanical design activities for the project include the cooling system, the containment structure, drive mechanisms for the control and transient rods, and the control rod design.

Task 5. Fuel Element Design (J. A. Reuscher, Supervisor)

This task interfaces with the fuel material development tasks (Tasks 6 and 7) and includes the stress analysis and heat transfer studies for design of the high-heat-capacity fuel elements. The fuel element demonstration tests are also a part of this task.

Task 6. Primary Fuel Material Studies (R. L. Coats, Supervisor)

The primary fuel material (at the present time) is $BeO-UO_2$ since it offers the largest performance improvement for the upgrade. This task involves the development of fabrication techniques, material compatibility studies, material property determinations, material analysis, and in-pile experiments for pulse testing of fuel geometries.

Task 7. Secondary Fuel Material Studies (C. H. Karnes, Supervisor)

The secondary fuel material is (UC-ZrC)-graphite which will be used in the high-heat-capacity fuel element if the BeO-UO_2 does not prove feasible. This task involves the development of fabrication techniques, material compatibility studies, material perperty determinations, material analyses, and in-pile experiments.

Task 8. Driver Core Fuel Element (J. A. Reuscher, Supervisor)

The testing of the outer core fuel material and the design of the driver core fuel element are the objectives of this task. This fuel is a uranium-zirconium hydride which is similar to the present ACPR fuel. The hydrogen-to-zirconium ratio is decreased slightly for the upgraded reactor. The testing of this fuel includes pellet tests and prototype element tests.

Task 9. Diagnostic System (J. E. Powell, Supervisor)

This task involves the development of a fuel motion detection system for fissile experiments in the upgraded ACPR. Such a system allows the detection of molten fuel motion in a reactor experiment. Several schemes are under development and involve both in-core and out-of-core devices. Progress on this task is reported as part of Sandia's Fast Reactor Safety Research Program (Ref. 7).

Project Schedule

The schedule for the ACPR Upgrade is shown in Figure 1. This figure gives the major events in the project and projects an operational date (critical experiment) about March 1978. A detailed PERT analysis of the overall project has been conducted, and the critical paths have been identified. The PERT chart is too detailed to include in this report.

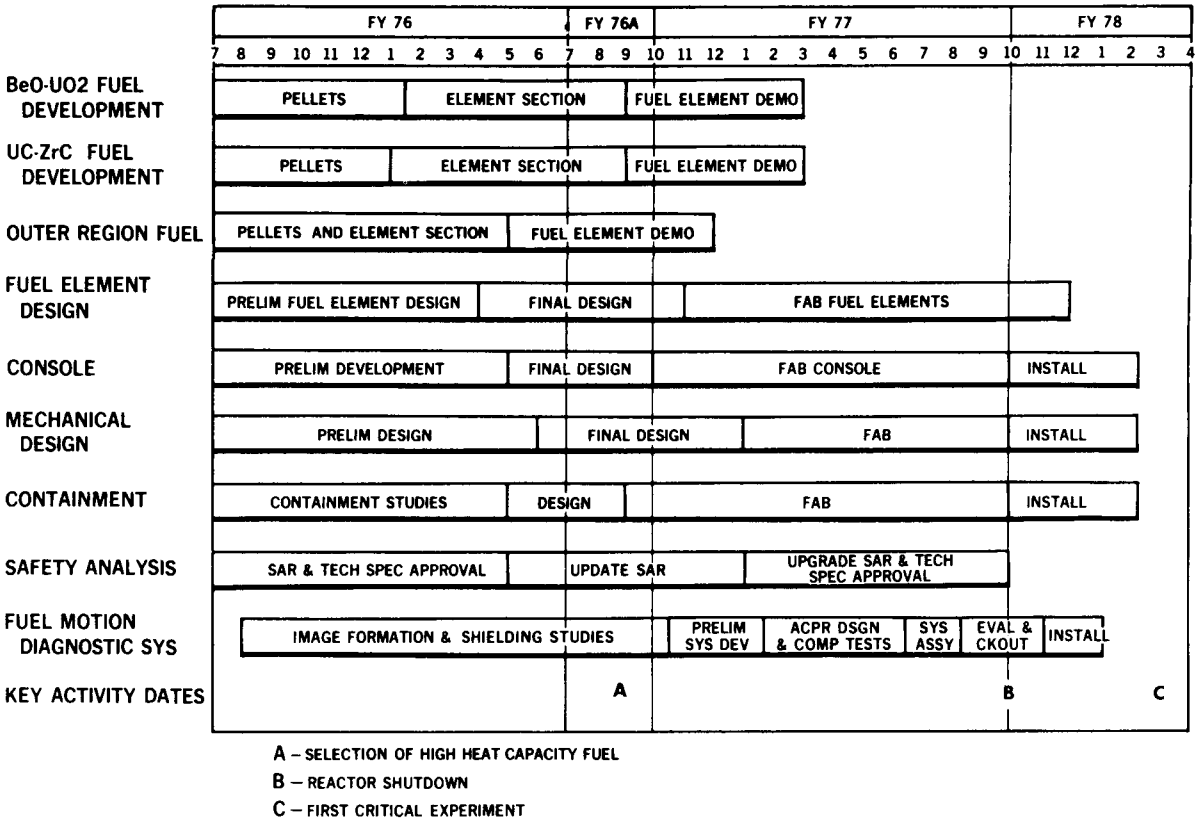

Figure 1. ACPR Upgrade Schedule

CHAPTER I

Task 1. Safety, Compliance, and Documentation

J. A. Reuscher, 5424; B. F. Estes, 5421

Introduction

This task involves the preparation of the safety documentation for the ACPR Upgrade, compliance with ERDA regulations concerning reactor design and construction, and planning for the initial tests and operations.

Safety Analysis Report (SAR)

During this quarter, the majority of the new chapters for the Safety Analysis Report were written in draft form. These chapters included Chapter 5 - Reactor Coolant System and Connected Systems, Chapter 6 - Engineered Safety Features and Chapter 8 - Electrical Power. The initial drafts of Chapter 4 - Reactor and Chapter 7 - Instrumentation and Control were about 50 percent complete.

Accident Analysis

The Accident Analysis chapter for the current ACPR SAR was examined by Intermountain Technologies, Incorporated of Idaho Falls, Idaho, for applicability to the upgraded reactor. Several of the analyzed accidents can be used directly for the new core; some of the accidents will require a reanalysis using design data for the two-region core. Other accidents not included in the present SAR but listed in Regulatory Guide 1.70, Revision 2, were considered. In addition, the reactivity effect of fissile material redistribution in the test cavity and the effect of failures in control element operations during transient modes were considered.

The Class 3 accident for the core was identified as a water-logged fuel element. Both high heat capacity fuels were examined for the possible consequences in an attempt to identify which one would produce the worst accident. There was insufficient data available to make a definite statement as to which fuel would create the worst water-logged accident. As a result, small-scale, water-logged tests are planned in the ACPR to identify the fuel which produces the greatest water vapor pressure for the same water mass and energy deposition. Some of the preliminary results from these experiments are reported in Chapter V.

A test apparatus was designed and built to measure the rupture pressure of the fuel clad. A seven-fuel element array was constructed so that a charge of black powder could be placed in the central fuel clad. The assembly was designed to be submerged in a water container which can be pressurized to the static pressure that exists at the core depth in the ACPR tank. The black powder will be ignited causing a rapid pressure rise in the clad and a transducer will measure the clad rupture pressure. Another transducer in the air space at the top of the test tank will measure the overpressure when the clad fails.

Quality Assurance Program

The Quality Assurance program for the ACPR Upgrade was developed and the chapter for the SAR was written. The program closely follows the Quality Assurance program utilized for the Sandia Pulsed Reactor III. The Design Review Committee was selected and a chairman identified.

CHAPTER II

Task 2. Core Nuclear Design
P. S. Pickard, 5424

The ACPR Upgrade core design studies have focused on two areas during the past quarter. The primary effort was directed toward the development of a suitable analytical tool for Upgrade kinetics studies. The second area of activity was the completion of preliminary neutronic designs for the UC-ZrC-C fuel candidate which included performance, kinetic analysis, detailed temperature effects, control rod worths, and reference experiment configurations in the Upgrade core. Comparative results have been obtained for the UO_2-BeO fuel candidate and these results are currently being evaluated and summarized. The development of a suitable space-time kinetics code for the Upgrade analysis was considered necessary because of the unique neutronic arrangement involved in the two-region core. The two regions have widely disparate, negative temperature characteristics and temperature distributions. The hydride fuel requires upscatter treatment for accurate results. The different fuel element types involved require a general heat transfer and temperature feedback capability.

The code currently being developed for this application utilizes cross section generation and collapsing routines written at Sandia, one-dimensional heat transfer and temperature feedback routines from Sandia, and the basic routines for space time kinetics from the GARIN-GASKIT codes. The cross section routines utilize standard ANSIN or DTF formats and allow an arbitrary energy group structure to be used for a given problem with the same basic library. Modification to the basic time-dependent diffusion algorithm include a generalized temperature feedback and cross section treatment, an acceleration technique for the predictors correction scheme and region-dependent axial leakage options. An implicit one-dimensional set of heat transfer routines was written for an arbitrary number of heat transfer models.

The heat transfer routines can also be run with point kinetics for survey calculations. The calculation begins with cross section generation, group collapsing, and steady-state calculations. The calculational sequence for the transient mode begins with cross section generation at a starting temperature and a one-dimensional diffusion calculation using the initial cross sections. This defines a heat generation rate which is then used in one-dimensional heat transfer calculations. The new temperatures generated are utilized to recompute cross sections for the next iteration.

Calculations performed with the one-dimensional, time-dependent code agree well with measured values for the current ACPR and with available static results for the Upgrade. A minimum of four energy groups are required to obtain reasonable results. (Special weighting functions can be used to improve results for fewer groups.)

Comparative results for the reactivity-temperature curve for both the current ACPR and the UC-ZrC-C Upgrade are shown in Figure 2. Typical pulse shapes for the ACPR and the UC-ZrC-C Upgrade are shown in Figure 3. A comparison of measured and calculated ACPR pulse characteristics are given in Table I.

The UC-ZrC-graphite fuel was chosen as a backup fuel candidate for the ACPR Upgrade and the majority of core design calculations have been completed for this fuel. A complete summary of both the UC-ZrC-graphite and UO_2-BeO will be included in the next quarterly report. The basic characteristics of the UC-ZrC-graphite core are summarized below. The basic core configuration consists of two rows of higher loading UC-ZrC-graphite fuel $\left(\approx 400 \frac{mg\ U^5}{cc}\right)$, a third row of lower loading UC-ZrC-graphite fuel $\left(\approx 200 \frac{mg\ U^5}{cc}\right)$ serving as a buffer zone, and three outer rows of $U\text{-}ZrH_{1.5}$ fuel of nominally 12 w/o U with 10 percent enrichment. The actual loadings in the three fuel regions depend on the upper temperature limit allowed for each fuel and the amount of U^{238} included in the fuel (enrichment). The additional Doppler feedback gained from additional U^{238}, coupled with a slightly shorter lifetime, allows a shorter risetime for a given pulse yield. The nature of this tradeoff is to reduce pulse fluence by about 5 to 10 percent, while reducing the pulse deposition time by approximately 15 to 25 percent.

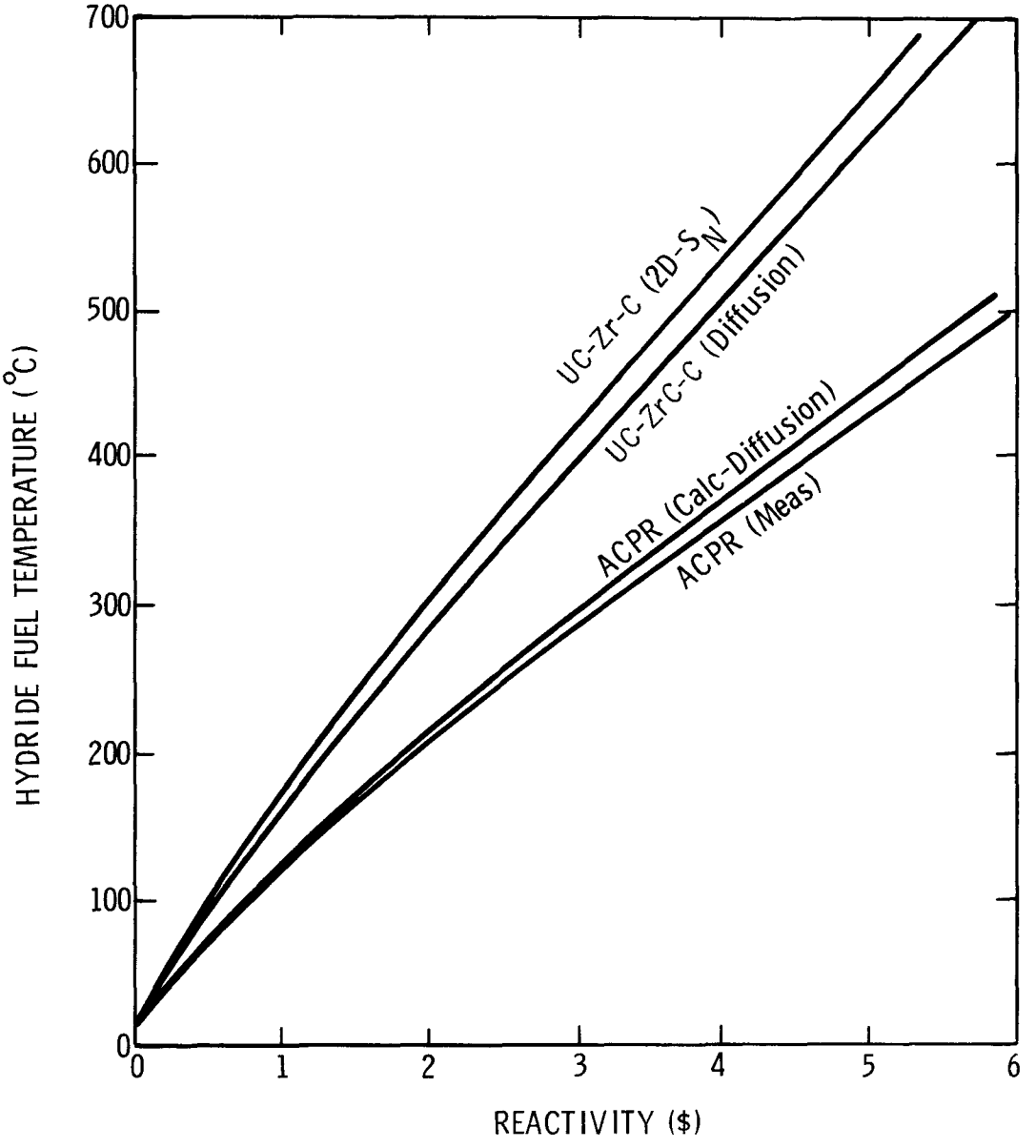

Figure 2. Reactivity Loss Curves for ACPR and UC-ZrC-C Upgrade

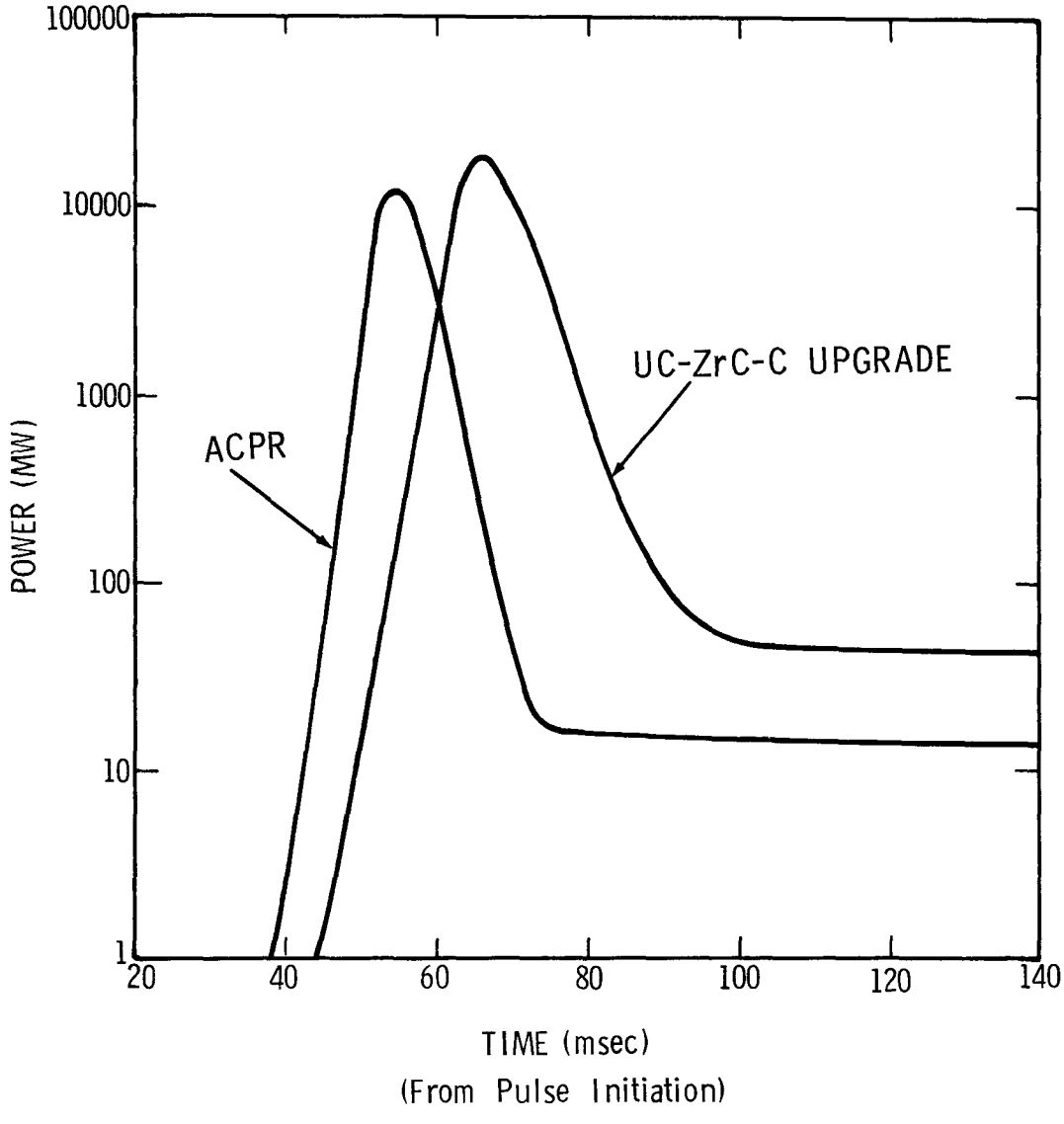

Figure 3. Comparison of Pulse Shape for Current ACPR and UC-ZrC-C Upgrade

TABLE I

Comparison of Measured and Calculated Kinetic Parameters

Parameter	ACPR (Measured)	ACPR (Calculated)
Maximum ΔT (^{o}C)	850^{o} C	850^{o} C
Fluence (n/cm^2)	2.2×10^{15}	2.2×10^{15}
Risetime (ms)	1.3	1.4
Tail Power Level (MW)	11	13
Yield (MW-s)	108	105
FWHM (ms) (2 x Front half width)	4.5	4.9

A parametric study (2D-S_N) for the shortest risetime UC-ZrC-C configuration is shown in Figure 4. Although an upper temperature limit has not been defined for the UC-ZrC-C, 2000^{o} C (adiabatic ΔT) was used for a reference core configuration with 7 percent excess Δk. The reference core loadings and characteristics are given in Table II.

Several variations of this reference core design have been analyzed and will be included in the final summary. These variations primarily involve alternative enrichments, relative region worths and control rod configurations. The summary of the UO_2-BeO studies and details of the reference core design will be included in the next quarterly.

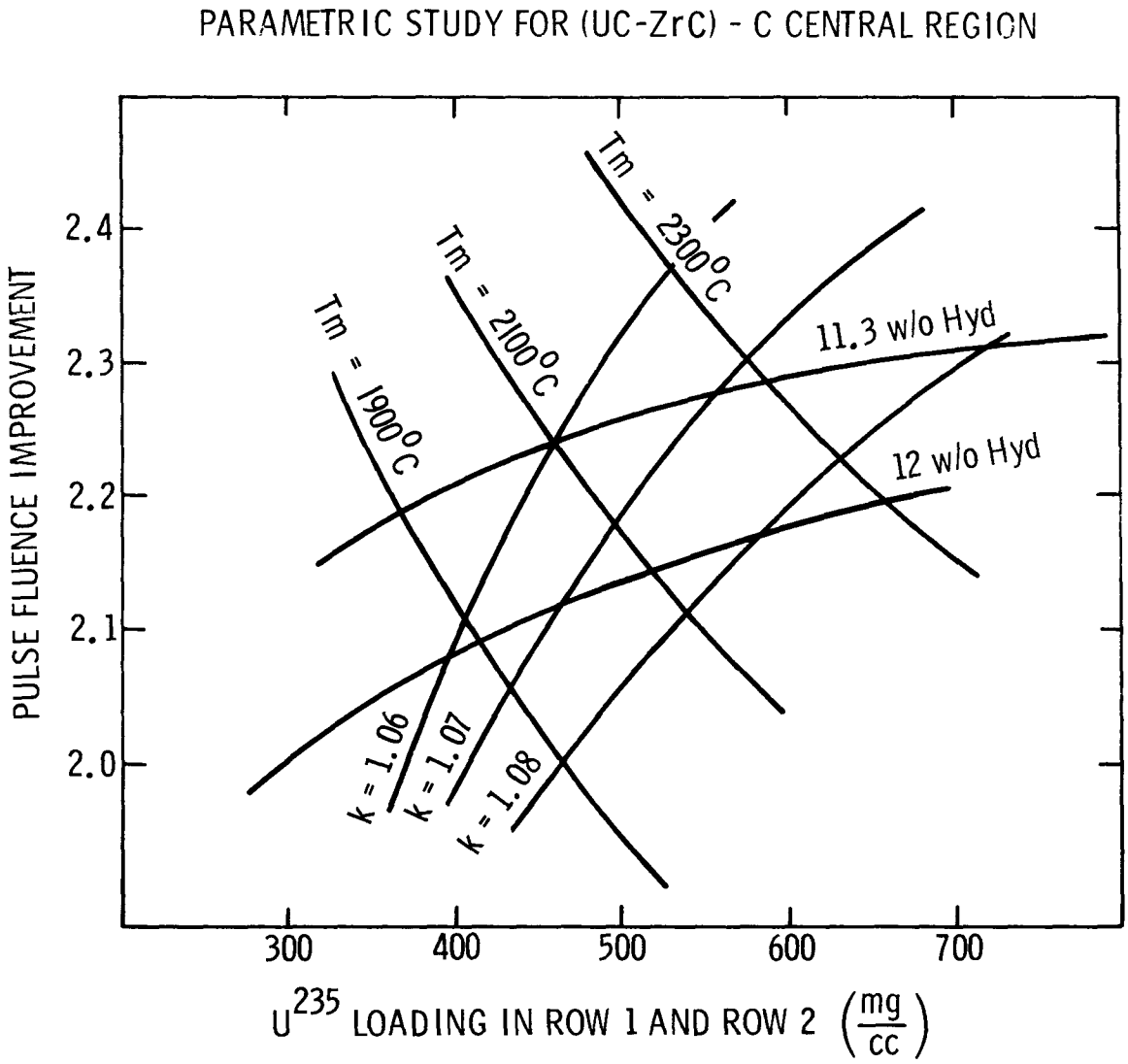

Figure 4. Performance Temperature Criticality Curves for Graphite-Hydride Two-Region Core

TABLE II

Basic Characteristics of UC-ZrC-C Reference Core

Parameter	Value for UC-ZrC-C Core
Loading R_1, R_2**	750 $\frac{mg\ U}{cc}$ - 60% U^{235}
Loading R_3	500 $\frac{mg\ U}{cc}$ - 40% U^{235}
Loading R_4, R_5, R_6	12.2 w/o U-$UZrH_{1.5}$ - 10% U^{235}
$\Delta T_{carbide}$	2000°C
$\Delta T_{hydride}$	1000°C
k	1.07
Performance Improvement --	
2000°C	2.1
2200°C	2.25
ℓ (μsec)	37 μsec
Temperature Coefficient (¢/°C) --	
23 - 200*	0.65
200 - 500*	0.79
500 - 900*	0.87
Minimum Period	1.9 msec
Yield (MW/sec)	250 MW/sec
Peak Flux ($n/cm^2/sec$)	10^{17}
Tail	45 MW
Steady State Flux --	
1.0 MW ($n/cm^2/sec$)	1.3×10^{13}
2.0 MW ($n/cm^2/sec$)	2.7×10^{13}

*Hydride Temperature

**R_1, R_2, etc., refers to the 1st, 2nd, etc., row of fuel elements radially outward from the irradiation cavity.

CHAPTER III

Task 3. Console Development
W. H. Sullivan, 5423

The system specifications for the ACPR Upgrade console were completed and submitted for quote on July 8, 1976. The quotation due date was August 9, 1976, but General Atomic requested, and was granted, an extension to August 23, 1976. The quote was received on August 26, 1976. The quoted price was substantially higher than our estimated price, and the quoted delivery was 15 months from receipt of order.

Both the delivery date and the quoted price are unacceptable. Preliminary discussions have shown that our specifications would require major redesign of at least three of their standard instrument channels, thus severely impacting both price and delivery. The specifications have been reviewed, and we can accept their standard instrumentation channels with no compromise to safety. The specifications are being revised to obtain a new price quote, and it is estimated that the savings will bring the cost within the original budget estimate and reduce the delivery time to the required 12 months after receipt of order.

CHAPTER IV

Task 4. Mechanical Design
D. K. Overmier, 1136A

Cooling System

Design of the system external to the tank has been completed. Action to purchase and install this portion of the system is being initiated.

Auxiliary Hoist

Preliminary design using a chain hoist has been completed. Subsequent efforts located a cable type hoist which is preferred on grounds of safety and length of lift; i.e., its drive train is non-overrunning and a 75-foot lift capacity (to reach tank bottom) is available. The original design will be modified to incorporate the cable hoist.

Ventilation System

The ventilation system design has been conducted through the preliminary stages. The need for such a system depends on the results of the accident analysis being conducted by Intermountain Technologies, Inc. To date, the primary technical question which has been identified involves the performance of the reactor tank exhaust system in the event of a water-displacing and/or vapor-generating accident in the core. Under normal operating conditions, it is assumed that the ventilation system will maintain a steady bleed flow of room air into the tank space between water surface and cover. This air will then be drawn off and exhausted through filters. The room air bleed valve will be controlled

to hold a specified pressure differential between the room and the tank space. The postulated accident would tend to pressurize the same space, thus requiring the air bleed be reduced or shut off to maintain the desired pressure differential. This dynamic response requirement on the bleed valve actuator and the air-moving device downstream of the filters depend heavily upon the time history assumed for possible events comprising the accident. The fact that an accident can be postulated which is capable of overpowering any realizable ventilation system requires the ground rules be established. Accordingly, efforts have been directed to developing a reasonable model of the system and a credible accident model. As it concerns ventilation system flow, the accident model must describe physically the material released and its progress from core to pool surface and to exhaust.

CHAPTER V

Task 5. Fuel Element Design

J. A. Reuscher, 5424; D. E. Lamkin, 5424;
F. M. Morris, 5424; H. E. Walling, 1136

Introduction

This task involves the design, testing, and procurement of the high-heat capacity fuel elements for the central region of the core The results of the in-pile fuel experiments are used to develop the fuel material and the fuel region configuration. The major activities for this quarter included steady-state heat transfer calculations for both the BeO-UO_2 and (UC-ZrC)-graphite fuel elements. In addition, the initial element section test experiments were conducted.

Heat Transfer Calculations

The twc-dimensional heat transfer code TAC-2D[8] was used with both the BeO-UO_2 and (UC-ZrC)-graphite fuel element designs. The basic BeO-UO_2 fuel element design is shown in Figure 5 and the various regions are identified in Table III. All dimensions are given in engineering units since these units are required as input to the heat transfer code. The design concept for the (UC-ZrC)-graphite fuel element is shown in Figure 6 and the various regions are identified in Table IV. The gap between the inside clad surface and the inner liner was varied to examine the effect on the element heat transfer characteristics.

The heat-transfer coefficient that was used at the clad/water interface was divided into three regions, depending on the clad temperature.

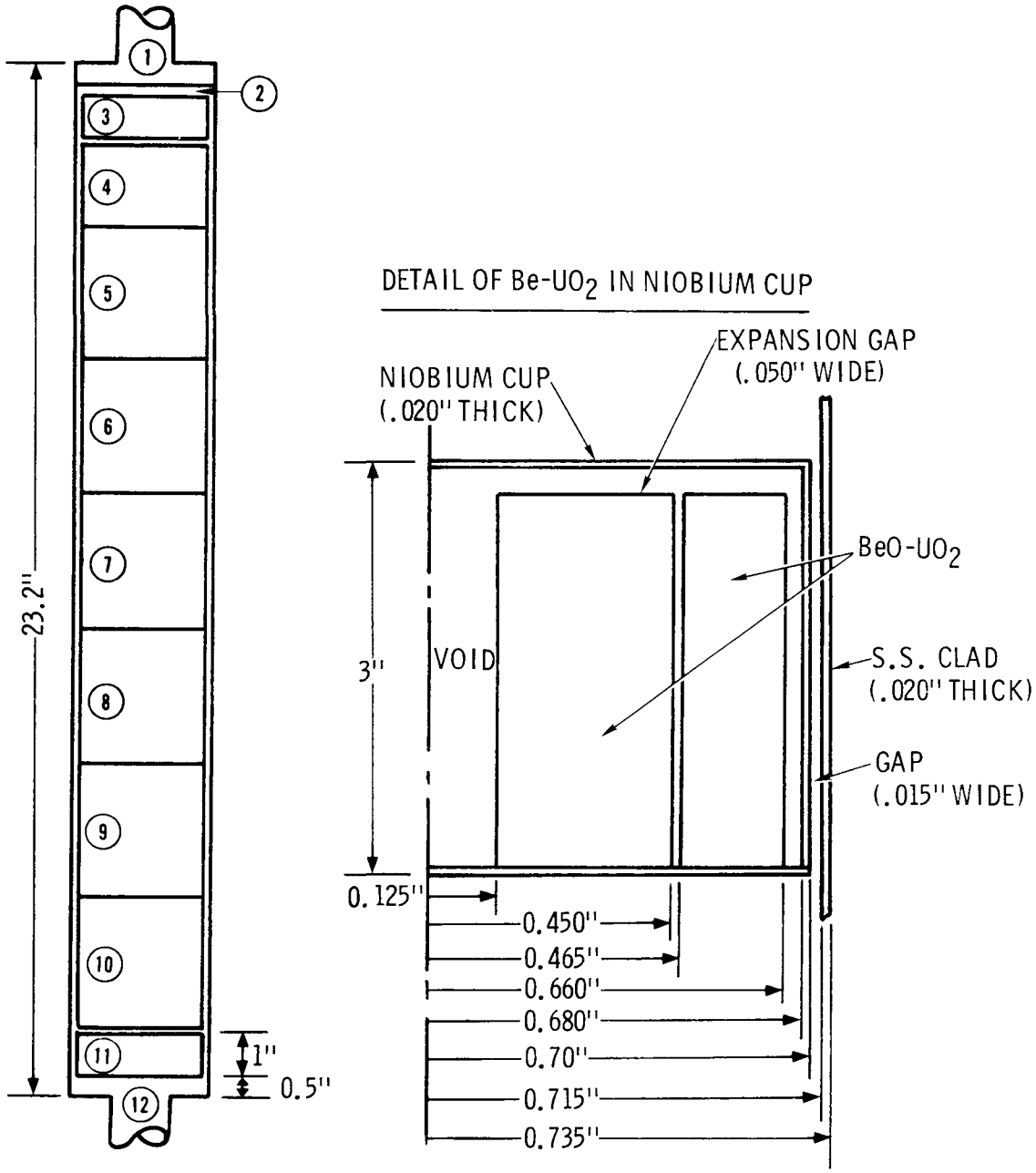

Figure 5. Be-UO_2 Fuel Element Design

TABLE III

Design Concept for $BeO-UO_2$ Fuel Element

Region	Description
(1)	Upper stainless-steel end fitting
(2)	0.23" wide expansion gap
(3)	BeO insulator, 1" thick, 1.43" O.D.
(4)	$Beo-UO_2$ fuel in niobium cup; length = ~2"
(5)	$BeO-UO_2$ fuel in niobium cup Length = ~3"
(6)	
(7)	
(8)	
(9)	
(10)	
(11)	BeO insulator, 1" thick, 1.43" O.D.
(12)	Lower stainless-steel end fitting

TABLE IV

Design Concept for (UC-ZrC)-Graphite Fuel Element

Region	Description
(1)	Upper stainless-steel end fitting
(2)	0.25" wide expansion gap
(3)	Graphite insulator, 1" thick, 1.4" O.D.
(4) thru (23)	(UC-ZrC)-graphite fuel region 1" long pellets, 1.3" O.D.
(24)	Graphite insulator, 1" thick, 1.4" O.D.
(25)	Lower stainless-steel end fitting

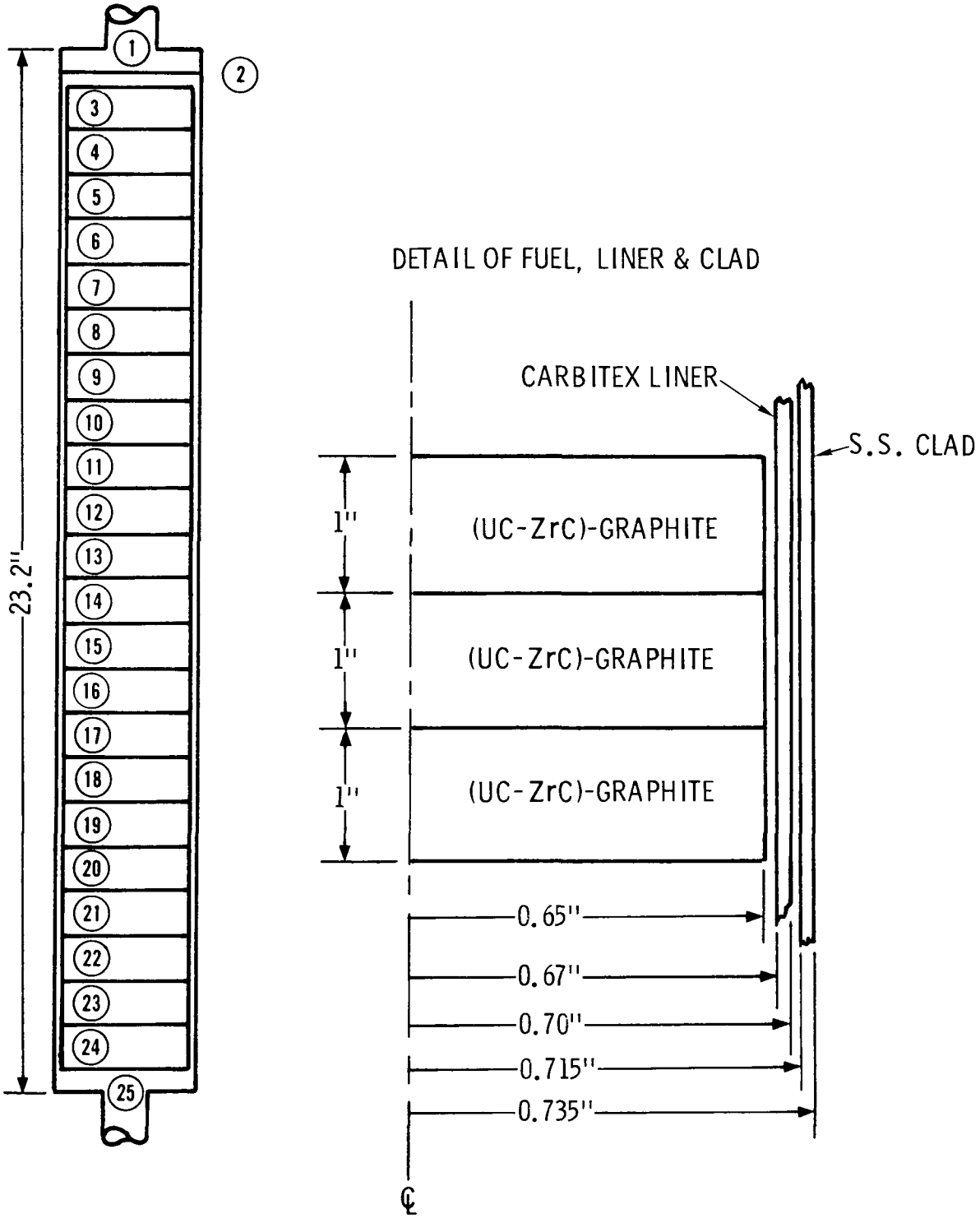

Figure 6. (UC-ZrC)-Graphite Fuel Element Design

that is,

$$h = 50 \text{ Btu/hr-ft}^2 - {}^{\circ}\text{R for } T_c \leq 530\ {}^{\circ}\text{R}$$

$$h = 50 + 0.294\ (T_c - 530) \text{ for } 530 < T_c \leq 700\ {}^{\circ}\text{R},$$

$$h = 100 + 4.173\ \frac{(T_c - 700)^3}{(T_c - T_w)} \text{ for } T_c > 700\ {}^{\circ}\text{R}$$

where

T_c = clad surface temperature

T_w = water temperature.

The heat transfer coefficient for nucleate boiling is based on the Rohsenow correlations. Note that 700 $^{\circ}$R is approximately the saturation temperature at the water depth of the core.

The temperature dependence of the thermal properties of the various materials in the fuel element designs was included in the calculations. Both steady-state and transient calculations were performed for both fuel element concepts.

The maximum BeO-UO_2 fuel temperature as a function of element power is shown in Figure 7 for three different gap thicknesses. The gap contains helium fill gas and the width is the distance between the niobium cup and the inside clad surface. An element power of 10 kW corresponds to a total core power of about 2 MW.

The maximum clad heat flux for both pulse and steady-state operation is given in Figure 8. The effect of gap thickness on heat flux for pulse operation is clearly shown; the steady-state heat flux is essentially independent of gap thickness. The Bernath[9] correlation for the departure from nucleate boiling is indicated. A pulse with a fuel temperature rise of 1300°C corresponds to an energy deposition of about 500 cal/g. This curve indicates that, with a gap width of 0.025 inch and a pulse of 500 cal/g, the clad heat flux is below the Bernath DNB. For a steady-state power of 10 kW, the heat flux is well below the DNB correlation.

The steady-state results for the (UC-ZrC)-graphite fuel element are given in Figure 9. The clad temperature is shown as a function of element power. The Bernath DNB clad temperature is 157°C and, for

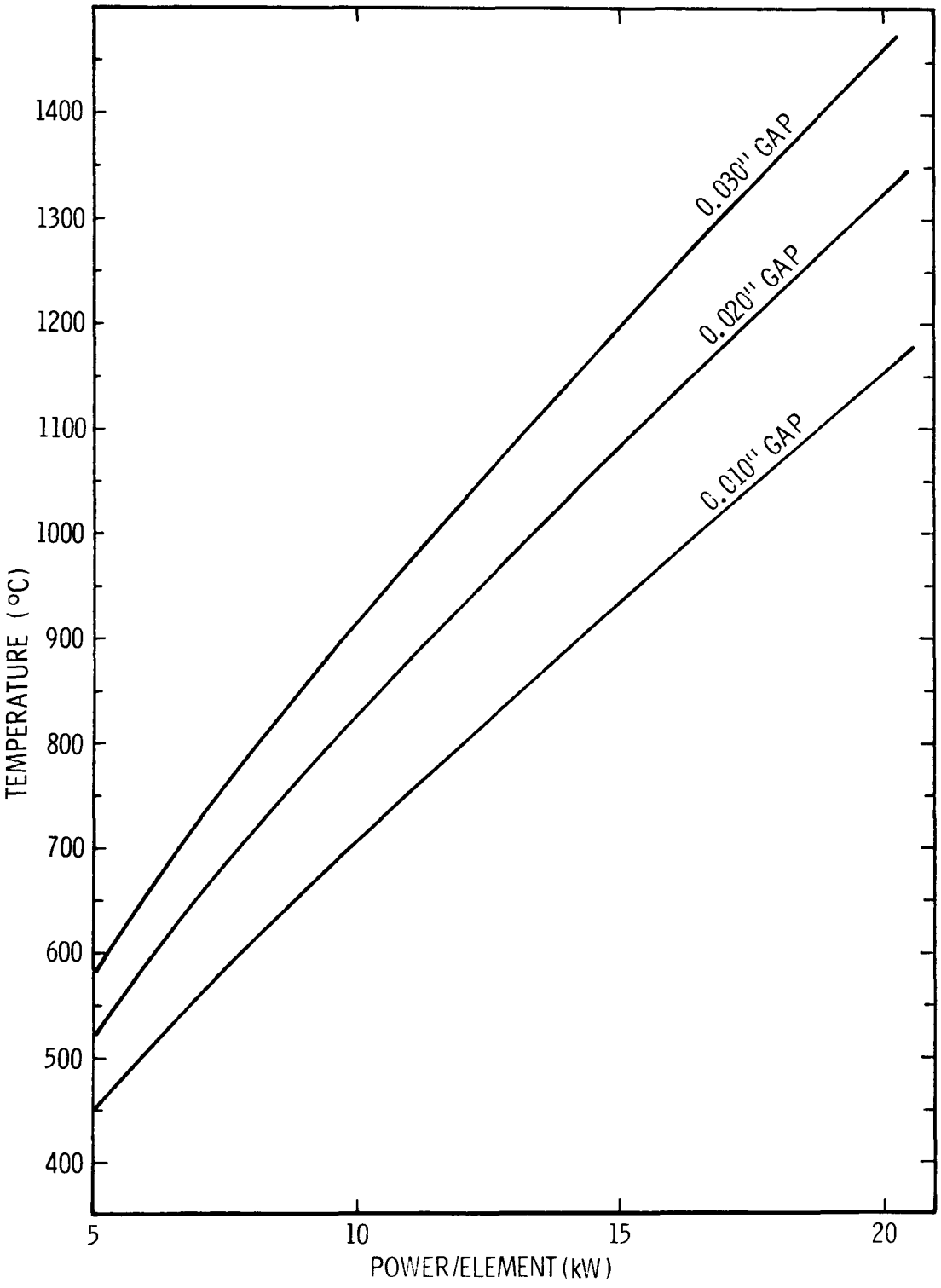

Figure 7. Steady State Operation - Maximum BeO-UO_2 Fuel Temperature versus Element Power and Gap Size

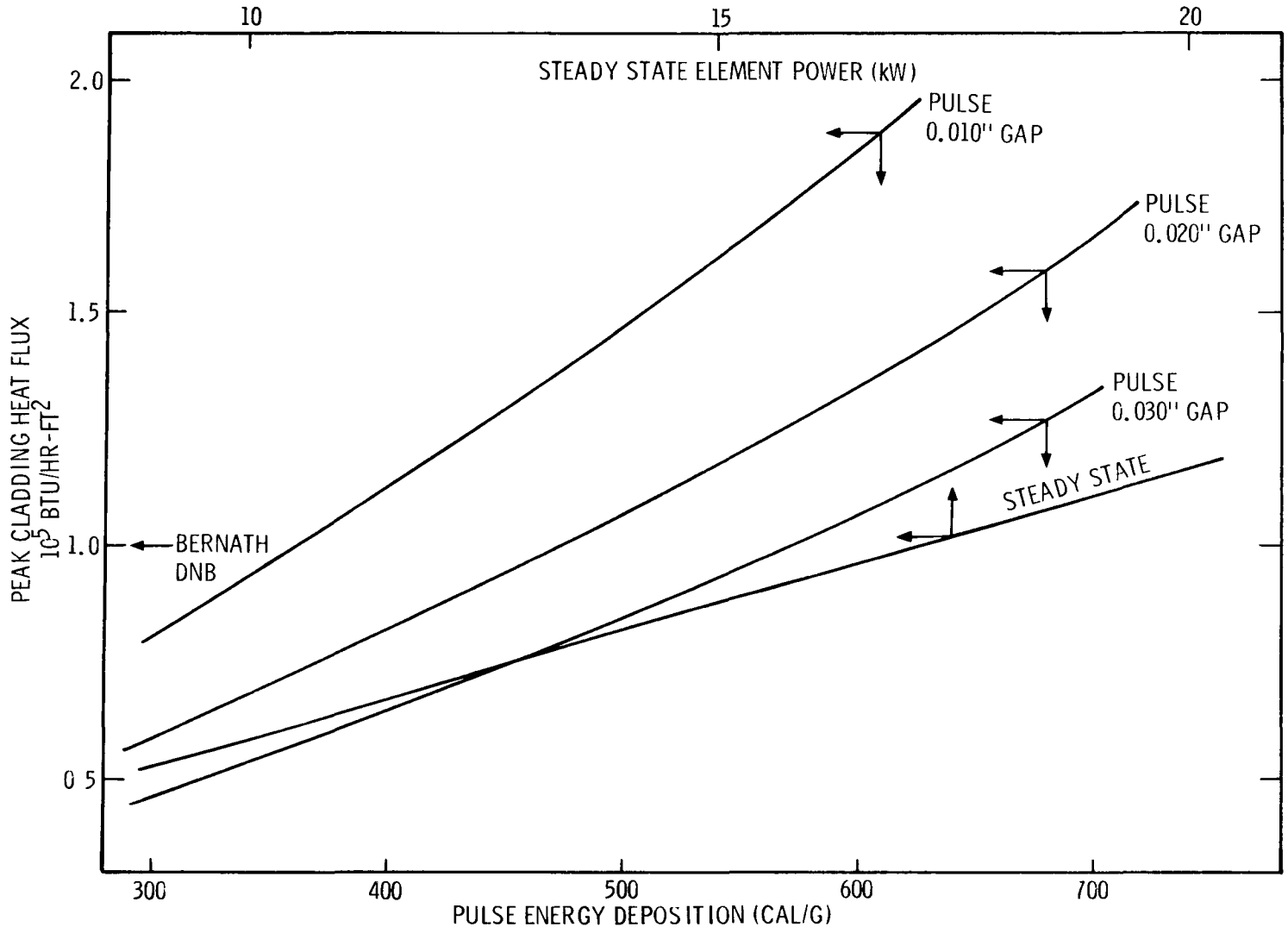

Figure 8. Peak Clad Heat Flux for Steady State and Pulse Operation for BeO-UO_2 Fuel Element

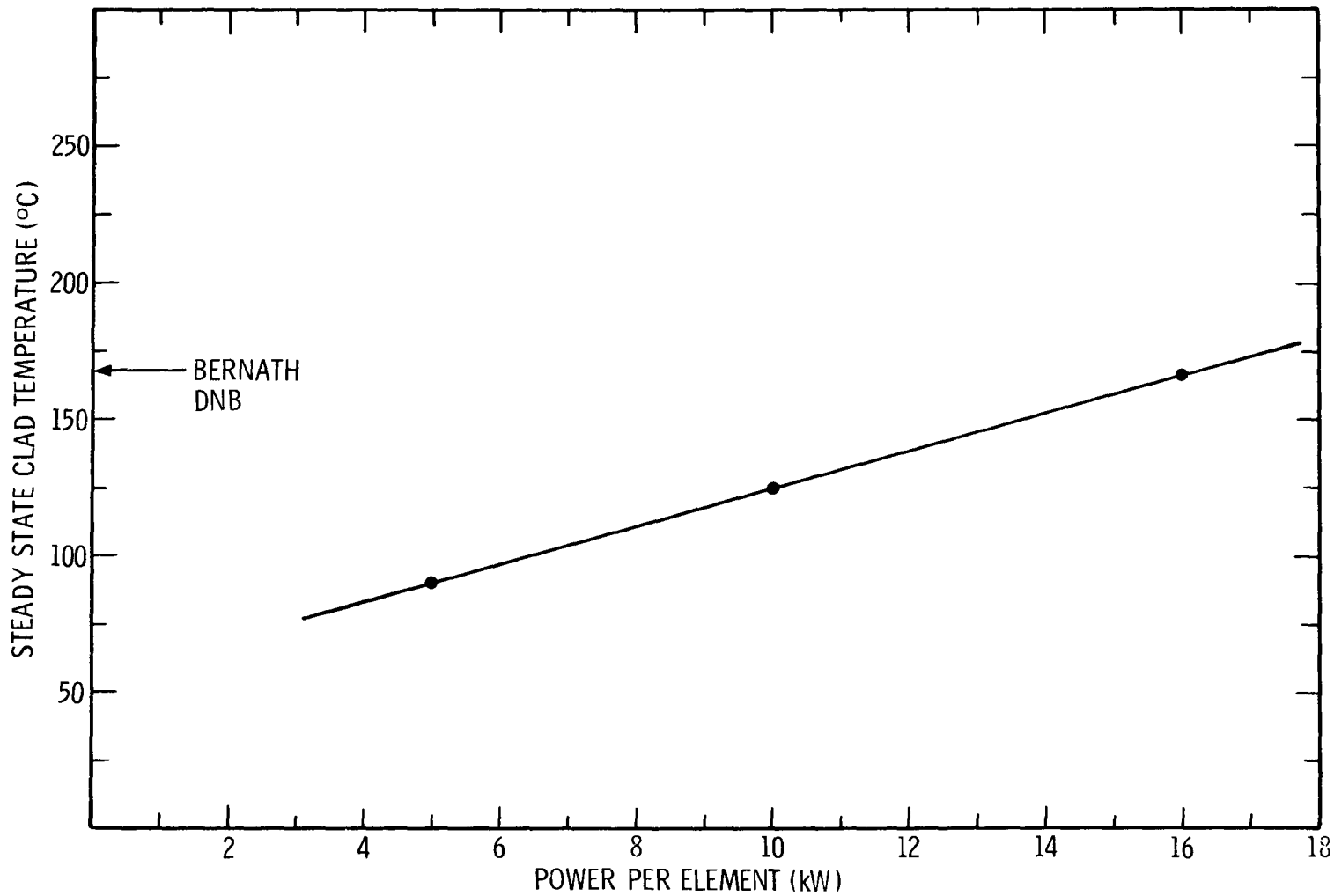

Figure 9. (UC-ZrC)-Graphite Fuel Element Clad Temperature versus Element Power

an element power of 10 kW, the temperature is about 125°C. An example of maximum fuel temperature as a function of element power is given in Figure 10 for a 0.015 inch helium gap. The effect of fuel conductivity is illustrated by the regions labeled low and high fuel conductivity. The regions were obtained by using several different heat transfer correlations at the clad/water boundary.

Element Section Test

The apparatus for the element section test is shown in Figure 11. A 20 cm long piece of dimpled clad was fabricated into a vessel by welding the lower end closed and attaching a threaded fixture to the upper end. The stainless steel vessel fits inside a 9 inch diameter aluminum vessel which is filled with 700 cc of water. The water thickness around the clad is about 1.9 cm. Two thermocouples are placed inside the clad and three thermocouples can be positioned outside the clad. In addition, the pressure inside the clad and in the water volume is measured. The energy depositions in the fuel are enhanced by up to a 2.5 cm thick polyethylene moderator placed around the outside of the experiment assembly.

The initial experiments were conducted with (UC-ZrC)-graphite containing a U-235 loading of 390 mg/cc. Four 2.5 cm long pellets were used with a Carbitex liner and thermocouples were spot welded to the outer clad surface. A thermocouple was also located near the center of the fuel stack and another was placed between the liner and clad. No polyethylene was used since the water provided the neutron moderation.

The maximum clad temperature as a function of average energy deposition is given in Figure 12. The peak fuel temperature achieved with this initial configuration was about 1280°C for an average energy deposition of 180 cal/g. Since the (UC-ZrC)-C fuel element temperature is expected to reach 2000° to 2200°C in the upgraded core, polyethylene was added to increase the energy deposition. With a 1.9 cm thickness of poly, the average energy deposition was increased by 30 percent; however, the temperature rise was still too low to properly simulate the fuel element behavior in the core. New fuel pellets with a U-235 loading of 600 mg/cc were ordered from Los Alamos Scientific Laboratory. The 600 mg/cc pellets should provide peak temperatures of about 2300°C in the (UC-ZrC)-C element section tests.

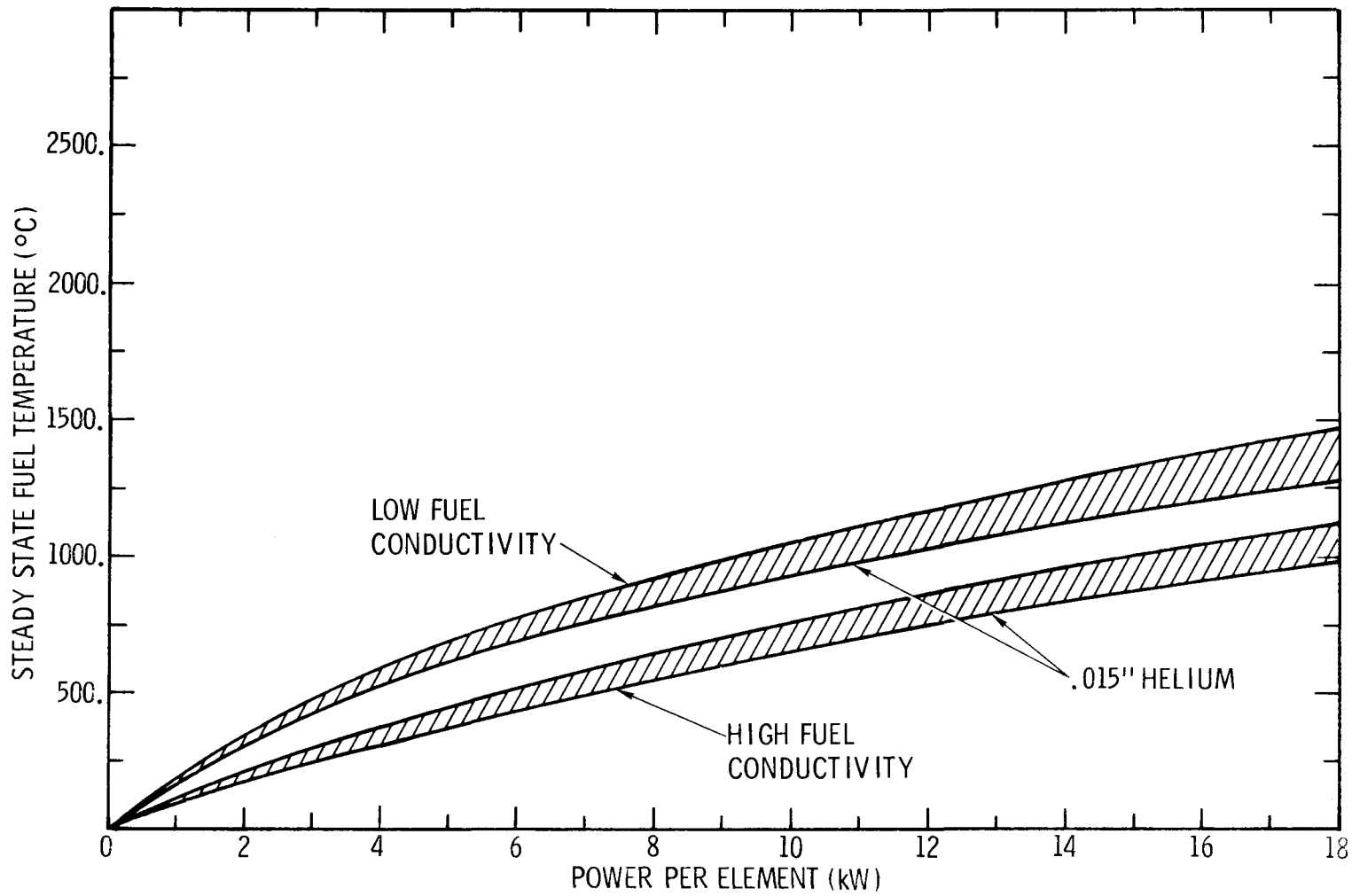

Figure 10. Effect of (UC-ZrC)-C Thermal Conductivity on Peak Steady State Fuel Temperature

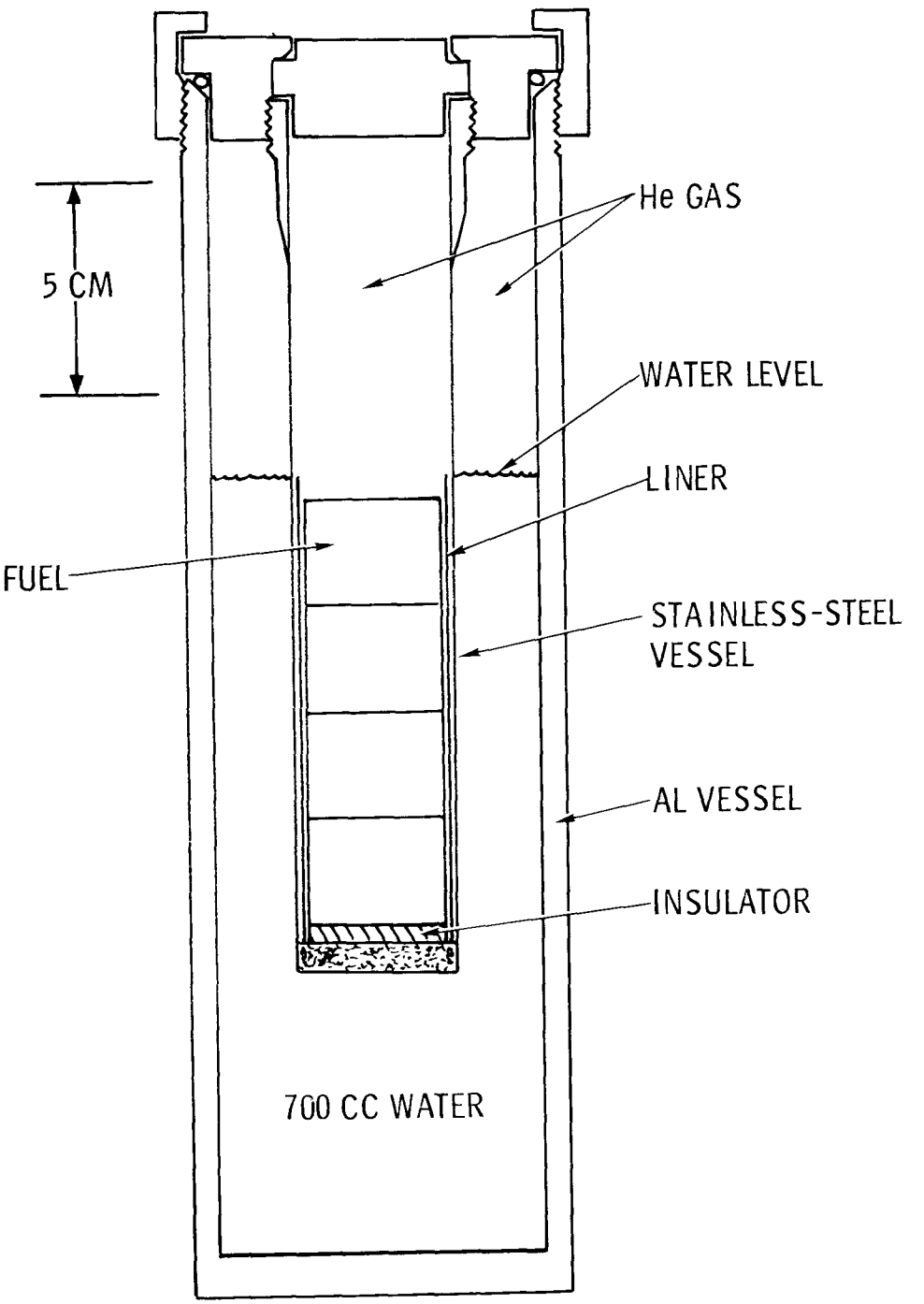

Figure 11. Element Section Test Apparatus

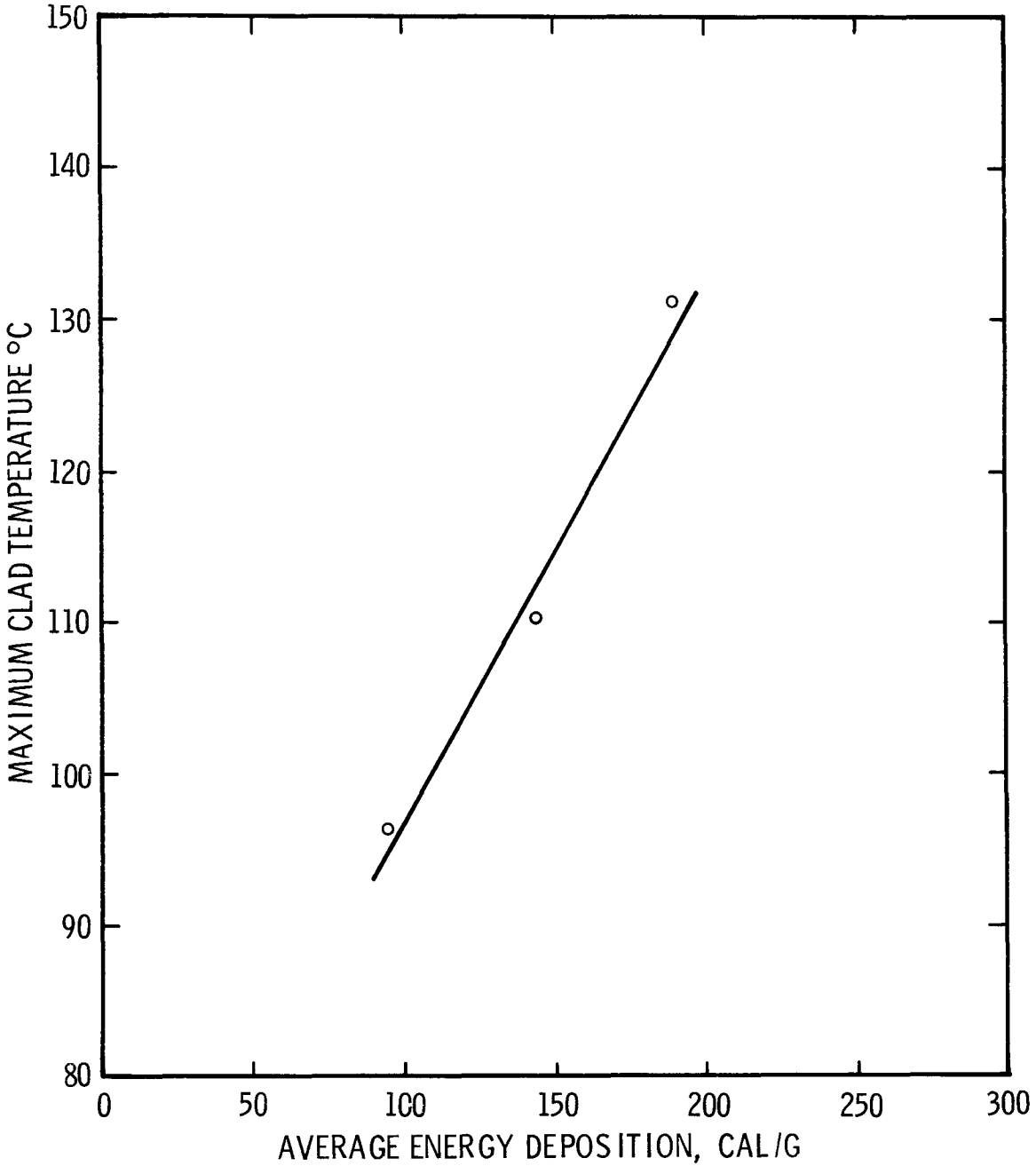

Figure 12. (UC-ZrC)-C Element Section Test Results

A limited number of $BeO-UO_2$ element section tests were conducted with 1.3 cm and 1.9 cm thicknesses of polyethylene and 700 cc of water. There was essentially no difference in the average energy deposition for the two poly thicknesses. The $BeO-UO_2$ contained 15 wt percent UO_2 and consisted of dual-slotted, concentric annuli; the pellets were placed in 5 cm long niobium cups. During this quarter, only the calibration pulses for the $BeO-UO_2$ element section test were conducted with a 50 percent reactor pulse. The data indicated that for a 100 percent pulse an average deposition of 360 cal/g ($\sim 1000^{\circ}C$) will occur in the outer annulus and 260 cal/g ($\sim 750^{\circ}C$) will occur in the inner annulus. A maximum surface temperature rise of 1150° to $1200^{\circ}C$ is expected. The results of the $BeO-UO_2$ experiments will be reported in the next quarterly report.

CHAPTER VI

Task 6. UO_2-BeO Fuel Development

D. J. Sasmor, 5422

Pulse Testing

The repetitive pulse testing of the BeO-UO_2 (15 wt% UO_2) dual slotted, dual annuli, cold-pressed and sintered fuel candidate was continued this past quarter. The testing at 1155°C was extended from 71 to 101 pulses and the testing at 1400°C was extended from 11 to 71 pulses. (See Table V.)

TABLE V

BeO-UO_2 Fuel Test
Cold Pressed and Sintered
¼-inch High Dual Slotted Outer Annuli

Repetitive Tests at 1155°C

Cumulative No. of Pulses	Samples Tested*	Cumulative No. of Fractured Samples*
1	8	0
11	8	0
31	8	0
51	8	1
71	8	2
101	8	2

Repetitive Tests at 1400°C

Cumulative No. of Pulses	Samples Tested*	Cumulative No. of Fractured Samples*
1	10	1
11	10	1
31	10	1
51	10	3
71	10	6

*Exclusive of end pairs.

Beryllium oxide-urania (12 wt%) with ternary additions have been exposed to single pulses ranging from 40 to 100 percent of maximum yield of the ACPR with 0.5 and 0.75 inches of polyethylene moderator. The samples tested were 0.25 inch high, 1.3 inch in diameter, and included (1) solid discs, (2) single annuli, 0.25 inch center hole, (3) single annuli, dual slotted. The fabrication methods and ternary addition combinations are as follows:

(1) Hot pressed with 20 volume percent niobium wire (.005" diameter)
(2) Cold pressed and sintered with 20 volume percent niobium powder
(3) Hot pressed with 20 volume percent niobium powder
(4) Hot pressed with 15 volume percent ZrO_2
(5) Cold pressed and sintered with 15 volume percent ZrO_2

Results of Testing

(1) Hot pressed with niobium fibers
The first visual observation of cracks in the solid discs was made after the 60 percent of maximum pulse (0.5 inch polyethylene moderator). The cracks extended through the ¼-inch thickness, but the wire reinforcement held the piece together. No additional cracks were observed in the subsequent tests. The dual slotted segments did not evidence any cracks through the full series of tests.

(2) Cold pressed and sintered with niobium powder
The solid discs of the material cracked severely at 80 percent maximum pulse with 0.5 inch polyethylene moderator and testing was discontinued.

(3) Hot pressed with niobium powder
Severe cracking of solid discs occurred at the 100 percent pulse with 0.5 inch polyethylene moderator.

(4) Hot pressed with ZrO_2
Severe cracking of the solid discs occurred at the 80 percent pulse with 0.5 inch polyethylene moderator.

(5) Cold pressed and sintered with ZrO_2
(a) Solid disc -- cracking of the solid discs did not occur through the 0.5 inch polyethylene moderated series of pulses 40 - 100 percent maximum ACPR yield. Severe

cracking was observed after the 100 percent ACPR (0.75 inch polyethylene) pulse.

(b) Single annuli -- cracks were discovered after the 100 percent pulse, 0.5 inch polyethylene moderator; no additional cracks were observed.

(c) Single annuli, dual slotted -- one half of one pellet was cracked at the 100 percent pulse (0.75 inch polyethylene moderator). The remaining pellets evidenced no damage.

Based on estimated peak temperatures for the various pulse-moderator combinations and calculated shape, temperature and stress curves, it appears that the cold-pressed and sintered $BeO-UO_2$ with 15 volume percent ZrO_2 added is capable of surviving approximately 30 percent greater stress than the cold-pressed and sintered $BeO-UO_2$ without ZrO_2. Dual annuli samples of cold-pressed and sintered material containing 14 volume percent ZrO_2 and 0.53 grams of urania per cubic centimeter is being fabricated for further test and evaluation.

Element Section Test

The fuel element section test (Cf Chapter V) of the $BeO-UO_2$ fuel has been initiated. Calibration pulses have been completed using 0.75 inch of demineralized water and 0.5-inch and 0.75-inch thick external polyethylene moderators. The dual slotted, dual annuli fuel pellets are stacked on a carbon support and are contained in two niobium containers (cups) which stack and nest (Figure 13). Two problems were encountered in placing the thermocouples in this system: (1) since it was not desirable to drill additional holes in the fuel, the fuel temperature thermocouple was placed between the halves of the inner annuli and hence, at best, yielded low temperatures; (2) the thermocouple, used to monitor the external surface temperature of the lower niobium cup, forces the column off center in the stainless outer clad resulting in metal-to-metal contact between the niobium cups and the stainless clad on the side opposite the thermocouple. Data from the test instrumentation are given in Table VI.

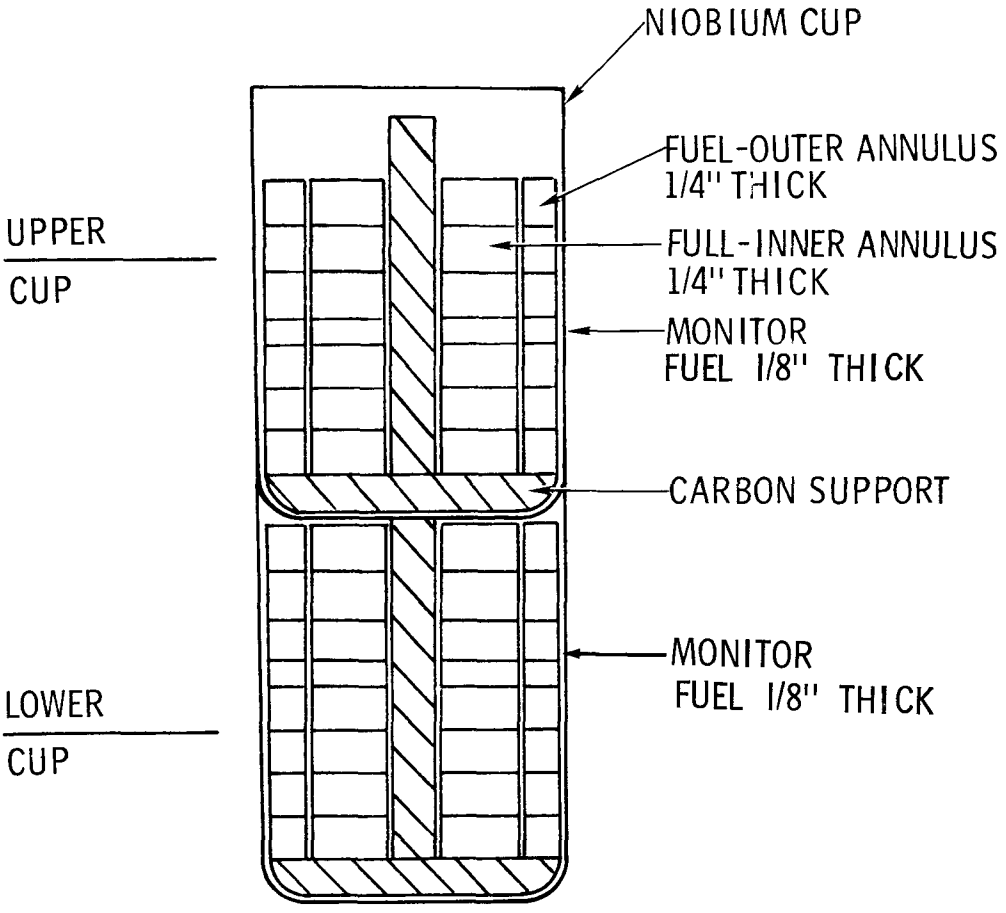

Figure 13. Stacked Niobium Cups with Fuel

TABLE VI

Fuel Element Section Test Results

	Series 1, #5 50% Max ACPR Yield 0.5" Polyethylene Moderator (External)	Series 1, #7 50% Max ACPR Yield 0.75" Polyethylene Moderator (External)
Fuel Temperature	342°C	342°C
Nb Clad Temperature	Thermocouple broken	250°C
Outer Clad Temperature, ΔT	72°C	77°C
Bulk Water Temperature, ΔT	49°C	58°C
ΔP Fuel Region, psi	14	16
ΔP Water Pressure, psi	3.5	4.1

Following the pulse, the experiment was disassembled and the average energy deposition in the fuel annuli was determined by fission product inventory. The energy deposition in cal/g for the individual annuli as a function of position are shown in Figures 14 and 15. The deposition profiles were determined by fission product counting of sections taken from the monitor pellets. The peak-to-average and peak-to-minimum depositions for the two tests are given in Table VII.

TABLE VII

Energy Deposition as a Function of Axial Position

		Test 1, #5	Test 1, #7
Peak/Average	Upper outer	1.398	1.221
	Upper inner	1.189	1.180
	Lower outer	1.266	1.249
	Lower inner	1.139	1.148
Peak/Minimum	Upper outer	1.529	1.462
	Upper inner	1.316	1.298
	Lower outer	1.538	1.559
	Lower inner	1.264	1.278

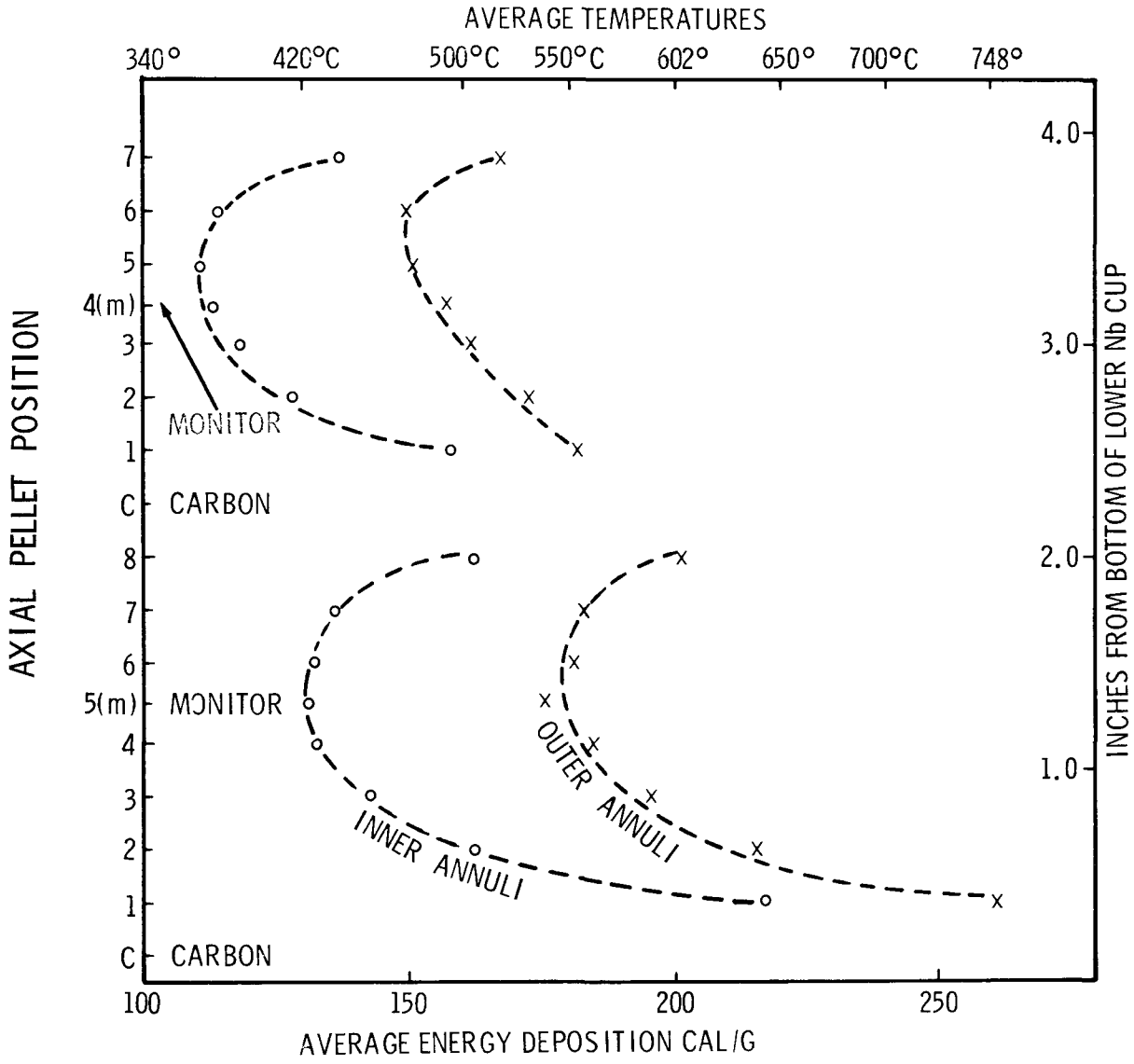

Figure 14. Series 1, Test #5 -- 700 ml Demineralized Water; 50 Percent Maximum Pulse; 0.5 inch Polyethylene

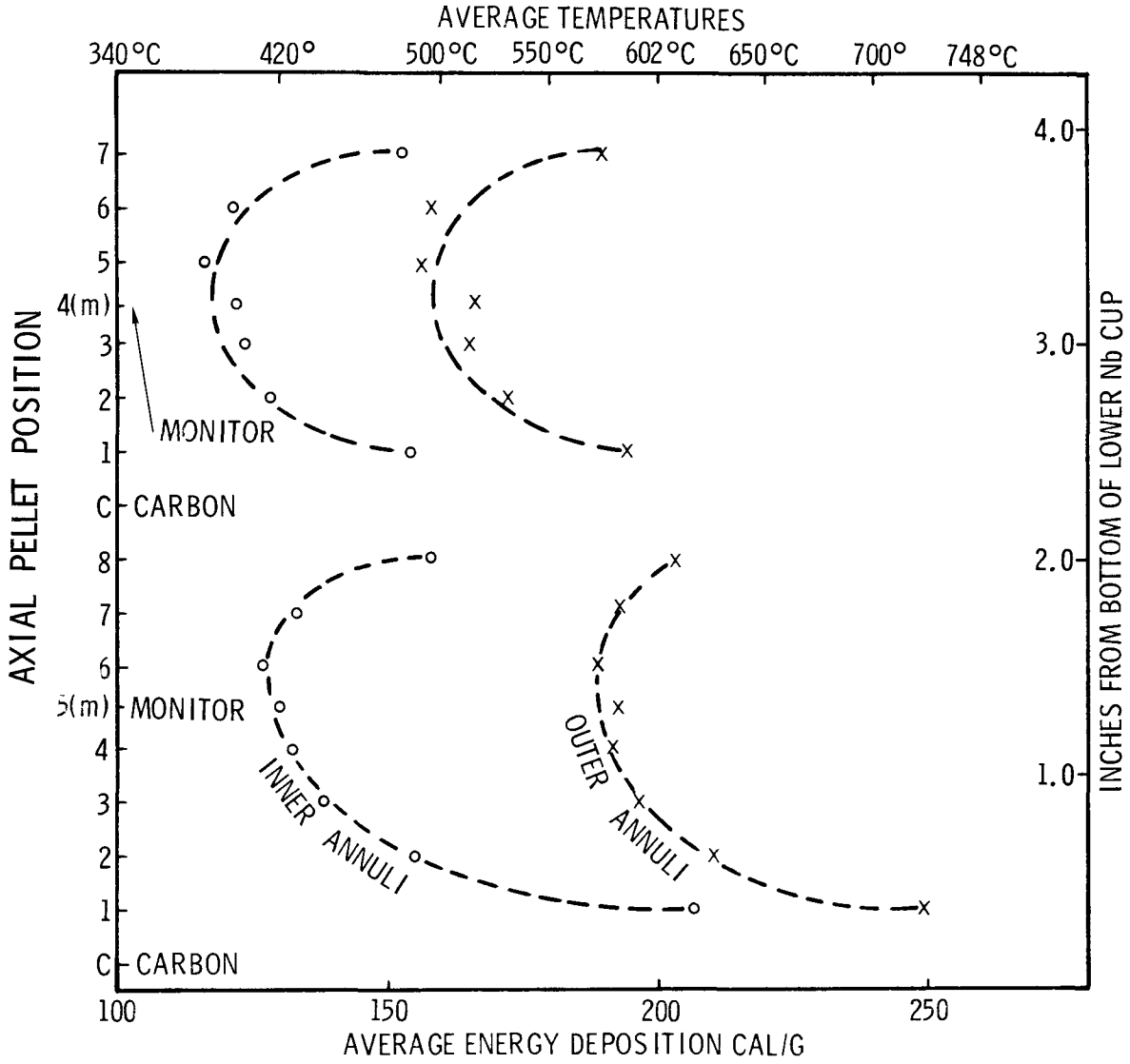

Figure 15. Series 1, Test #7 -- 700 ml Demineralized Water
50 Percent Maximum Pulse, 0.75 inch Polyethylene

The calculated adiabatic surface temperatures (average temperature (P/A) of the outer annuli in Test #5 range from 660°C to a high of 950°C and in Test #7 from 600° to 900°C.

Compatibility Studies

Samples from the initial compatibility tests of BeO-UO_2-niobium have been examined optically and with the Scanning Electron Microscope (SEM). Samples of niobium sheet and BeO-UO_2, and BeO-UO_2 with niobium fibers (0.005" diameter) in an alternate stack geometry were heated to 1275° - 1300°C in vacuum for periods of 4 to 24 hours. Samples were removed from the test at 4, 8, 16, and 24 hours. There was no adherence between the ceramic sample material and the niobium sheets. Optical and SEM examination of polished sections of the samples showed no evidence of interaction between the BeO-UO_2 and the niobium. Data from energy dispersion x-ray analysis provided additional evidence that there was no interaction.

Of particular interest are the hot-pressed samples of BeO-UO_2 with niobium fibers. This material was hot pressed at 1470°C for one hour in an argon atmosphere. Figure 16 is a SEM of the as-received sample, and Figure 17 is an elemental distribution photograph of the niobium. Figure 18 and 19 are photographs of a sample of the same material which was heated for 4 hours at 1275° - 1300°C. There is no evidence of interaction or diffusion of the materials. (Note: The uranyl nitrate solution used in manufacture of the BeO-UO_2 is reported to contain 50 ppm of niobium.) The niobium which appears in the ceramic body in the elemental distribution photograph is assumed in part to be from this impurity and/or from the smearing of the specimen surface during polishing). Further compatibility tests at 1500°C and 1800°C are planned.

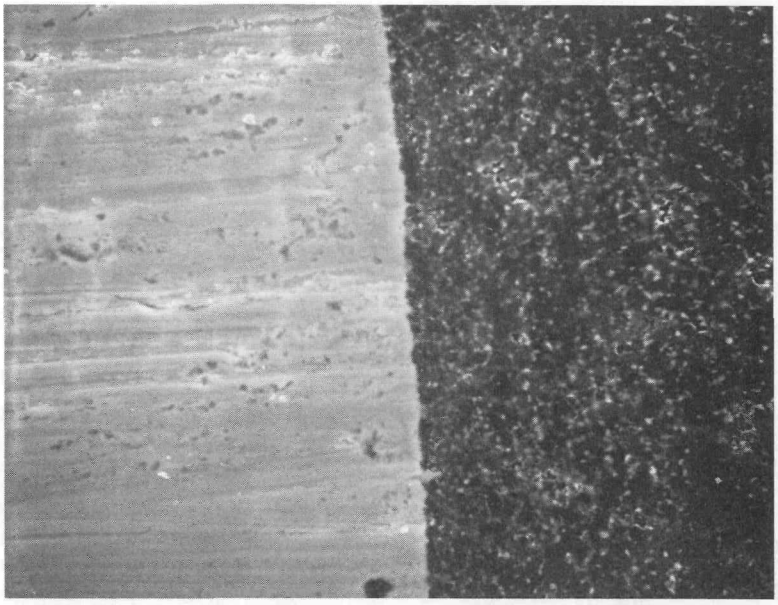

Figure 16. SEM of As-Received Hot Pressed BeO-UO_2 Sample

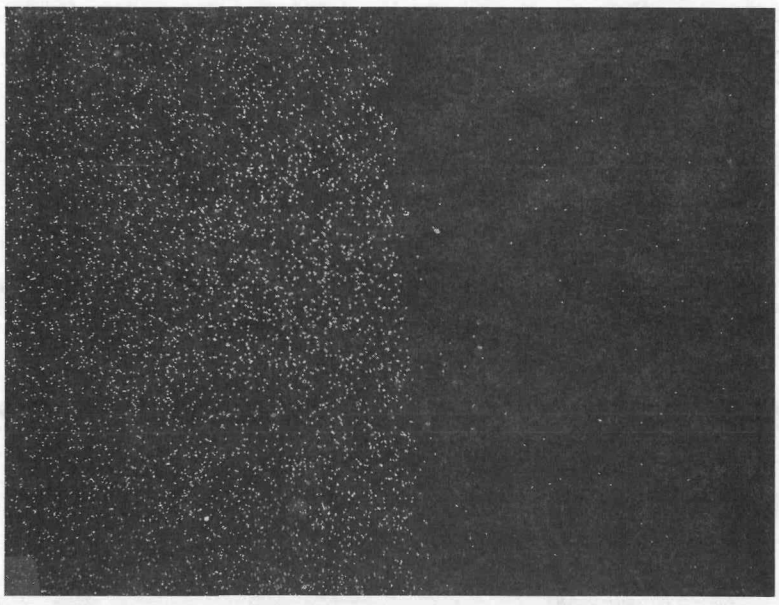

Figure 17. Niobium Map of Figure 16

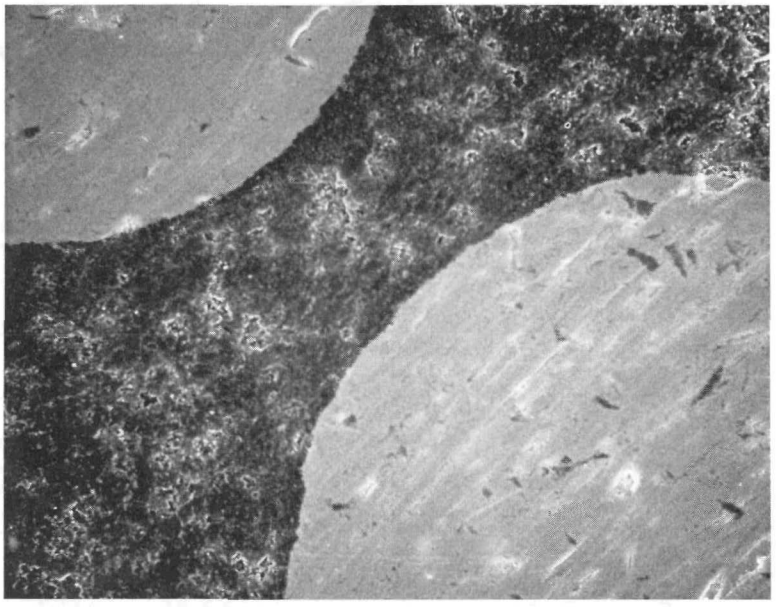

Figure 18. SEM of Heat Treated BeO-UO_2 Sample

Figure 19. Niobium Map of Figure 18

CHAPTER VII

Task 7. Secondary Fuel Material Studies

R. H. Marion, 5847; C. H. Karnes, 5847

Introduction

The fabrication and characterization studies of experimental lots of graphite-matrix fuel have continued during this reporting period. The new materials received will be described and the results of characterization studies will be presented according to technique, rather than material. The reader is referred to past quarterly reports for information pertaining to previously characterized fuels.

Lots SL018, SL019, and SL021 were fabricated and received, and are described in Table VIII. Lot SL018 contains 15 volume percent HMS graphite fibers which were originally 7.5 μm diameter and 250 μm long. The fibers are not visible in the photomicrograph in Figure 20a, but etching reveals them to be badly broken and they are probably not very effèctive as reinforcements. This material was hot pressed at 2500°C and 24 MPa (3500 psi). The (U,Zr)C solid solution has a desirable discontinuous structure with particles being less than 20 μm across.

Lot SL019 contains the very small graphite flour which resulted in the low porosity. The carbide distribution as shown in Figure 20b is similar to that of Lot SL018 and others previously reported. It was hot pressed at the same conditions as the previously reported Lot SL007.

Lot SL021 was hot pressed at 2350°C; otherwise the fabrication conditions were also the same as Lot SL007. The carbide distribution seen in the photomicrograph in Figure 20c indicates that all of the carbide particles are less than 20 μm and most of them are less than 10 μm.

TABLE VIII

Lot Identification

Lot	Process/ Geometry	Density (g/cc)	Porosity (%)	Carbide Content (vol %)	U Loading - 93% Enriched (mg U/cc)	Type of Graphite Flour	Size of Graphite Flour (μm)
SL001	Extruded/ Solid	3.497	22.6	34.8	434	KX-88	< 75
SL002	Extruded/ Solid	3.538	23.3	35.1	509	KX-88	< 75
SL003	Extruded/ Outer Dual Annulus	3.560	18.6	35.8	332	KX-88	< 75
SL004	Extruded/ Inner Dual Annulus	3.545	21.8	35.1	491	KX-88	< 75
SL007	Hot Pressed Solid	3.55-3.80	10.0	31.8	359	KX-88	< 45
SL008	Hot Pressed Solid	3.32-3.78	20.0	33.1	383	KX-88	< 45
SL012	Extruded/ Inner Dual Annulus	3.414	19.4	30.2	519	9553	< 45
SL013	Extruded/ Outer Dual Annulus	2.826	21.6	20.1	345	9553	< 45
SL015	Hot Pressed Solid	3.597	~8	29.4	435	9553	< 45
SL017	Extruded/ Solid	2.69	23.4	16.7	420	9553	< 45
SL018	Hot Pressed Solid W/Fibers	3.50	10.0	29.2	432	9553	< 45
SL019	Hot Pressed Solid	3.776	4	31.9	453	9553	< 10
SL021	Hot Pressed Solid	3.024	10	17.1	423	9553	< 45

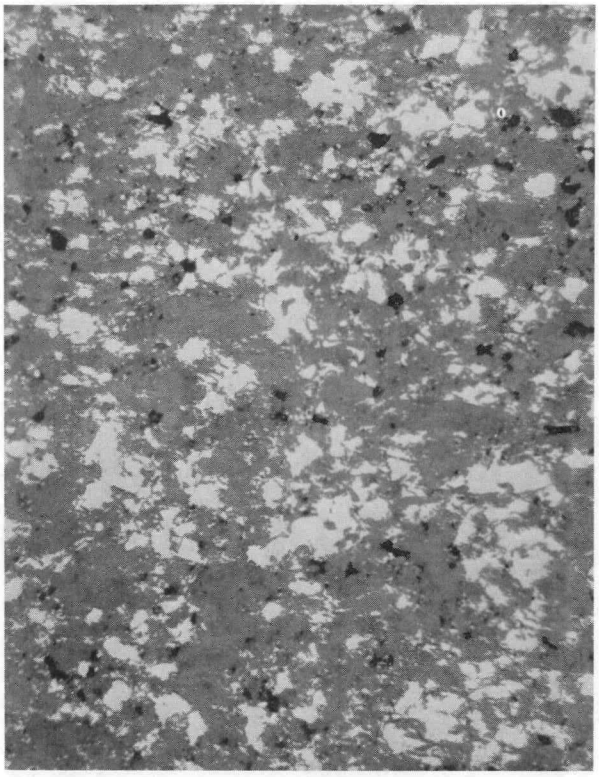

(a) Lot SL018 250X

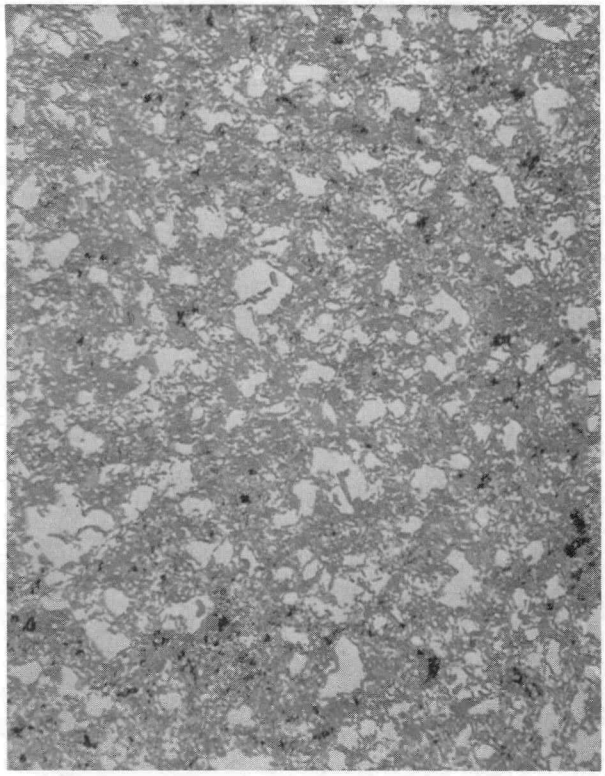

(b) Lot SL019 250X

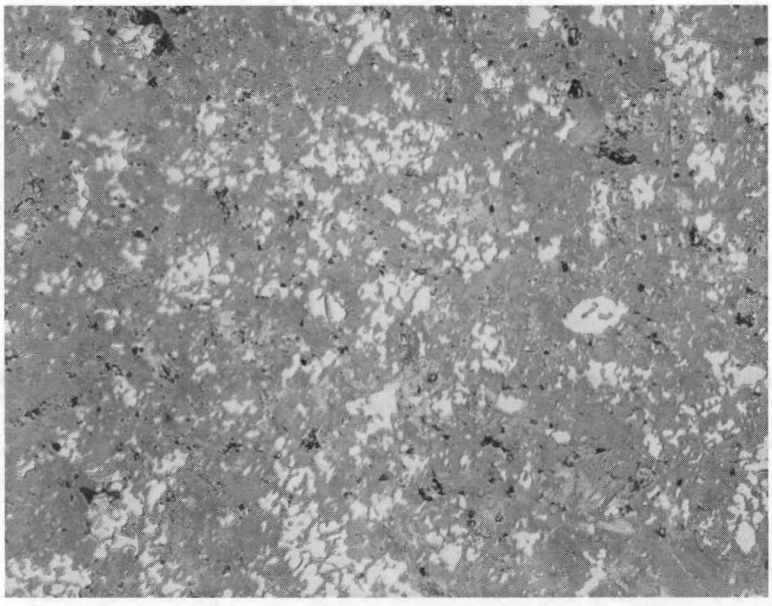

(c) Lot SL021 250X

Figure 20. Photomicrographs of Graphite-Based Fuel Fabrication and Characterization Studies

Reactor Pulse Test Results

Pellets from Lot SL018 (hot pressed with fibers) were tested in the ACPR under 100 percent pulses. A test of one 1.0-inch and two 0.5-inch high pellets resulted in a 0.5-inch high end pellet cracking after only one pulse. This pellet was replaced and the stack subjected to five full pulses. All pellets survived. Lot SL019 pellets (hot pressed with < 10 μm of 9553 graphite flour) were subjected to a full pulse. The test contained one 1.0-inch and two 0.5-inch high pellets; the 0.5-inch end pellet fractured and an obvious flaw was revealed.

Thermophysical Properties

Thermal expansion coefficients of fuels through Lot SL019 have been determined and are presented in Table IX. Note that Lots SL013 and SL017 have expansion coefficients which are considerably lower than the others. These two lots are materials which have low carbide content and, therefore, should perform better in a thermal stress environment.

The thermal diffusivities of these materials have been determined by the pulsed laser method and the results are presented in Table X. The low carbide content fuels (Lots SL013 and SL017) have a considerably higher diffusivity but the difference decreases at higher temperatures.

As previously reported, the experimentally determined heat capacity and enthalpy values for samples from Lots SL002 and SL013 (extruded materials) agreed with calculated values within four percent. A check has been made on samples from Lot SL008 (hot pressed material), and it was found that calculated and experimental values of enthalpy agreed within one percent. It is concluded that no further measurements of enthalpy are necessary.

Mechanical Properties

The fracture strength, fracture strain, and elastic modulus obtained as a function of temperature for Lots SL017, SL018, and SL019 are presented in Tables XI, XII, and XIII. As noted, some of the specimens broke in the grips resulting in only an indication of the fracture strength and fracture strains.

TABLE IX

Thermal Expansion

Lot #	$\bar{\alpha}$ 20-1500°C ($\times 10^{-6}/°C$)	$\bar{\alpha}$ 20-2000°C ($\times 10^{-6}/°C$)
SL001	6.6	6.9
SL002	6.6	6.8
SL003	6.7	---
SL007, SL008	7.2	7.3
SL012	5.8	5.8
SL013	4.3	---
SL015	7.7	9.4
SL017	4.4	4.7
SL018	8.5	---
SL019	8.1	---

TABLE X

Thermal Diffusivity
(cm^2/sec)

Lot #	300°C	820°C	1450°C	1835°C
SL001	.162	.110	.099	.093
SL002	.181	.125	.106	.100
SL003	.164	.115	.105	.092
SL004	.142	.105	.099	.094
SL007, SL008	.127	.093	.084	.082
SL012	.184	.126	.115	.107
SL013	.224	.146	.125	.108
SL015	.128	.095	.080	.077
SL017	.291	.187	.145	.122
SL018	.117	.092	.074	.166

TABLE XI

Mechanical Properties of Lot No. SL017

Sample Number	Test Temp (°C)	Fracture Strength MPa (psi)	Fracture Strain (%)	Initial Modulus GPa (10^6 psi)
SL017-089-3-1	22	35.3 (5130)	0.26	17.2 (2.5)
-4-1	22	32.7 (4750)	0.23	18.9 (2.75)
-3-2	1000	32.2 (4680)	----	----
-4-2	1010	37.5 (5090)	0.25	15.1 (2.2)
-3-3	1480	37.2 (5400)	0.25	15.1 (2.2)
-4-3	1475	37.0 (5380)	0.28	15.1 (2.2)
-3-4	1950	> 15.3 (> 2220) †	> 0.13 †	13.1 (1.9)
-4-4	1990	33.3 (4830)	0.70	6.9 (1.0)
-4-6	1950	> 30.7 (> 4460) †	> 0.35 †	11.7 (1.7)
-3-5	2390	> 15.0 (> 2180)	> 0.60 †	4.1 (0.60)
-4-5	2390	16.5 (2390)	1.00	3.7 (0.54)

† Broke in grip

TABLE XII

Mechanical Properties of Lot No. SL018

Sample Number	Test Temp (°C)	Fracture Strength MPa (psi)	Fracture Strain (%)	Initial Modulus GPa (x 10^6 psi)
SL018-0115-1	22	20.2 (2930)	0.17	15.2 (2.2)
-0117-3	22	24.9 (3610)	0.28	13.1 (1.9)
-0121-2	22	23.5 (3410)	0.23	13.8 (2.0)
-0115-2	1000	31.0 (4500)	---	---
-0120-1	990	33.0 (4790)	---	---
-0115-3	1470	23.8 (3460)	0.50	8.3 (1.2)
-0120-2	1480	27.6 (4010)	0.25	9.0 (1.3)
-0117-1	1940	19.4 (2810)	0.65	4.34 (0.63)
-0120-3	1970	26.7 (3870)	---	---
-0117-2	2390	9.1 (1320)	1.40	1.2 (0.17)
-0121-1	2370	3.9 (560)	0.70	0.7 (0.10)

TABLE XIII

Mechanical Properties of Lot No. SL019

Sample Number	Test Temp (°C)	Fracture Strength MPa (psi)	Fracture Strain (%)	Initial Modulus GPa (x 10^6 psi)
SL019-0146-1	22	20.6 (2990)	----	----
-0149-1	22	22.7 (3300)	0.13	17.9 (2.6)
-0151-3	22	> 19.0† (> 2750)	> 0.12†	19.3 (2.8)
-0146-2	1025	18.5 (2690)	----	----
-0148-3	1015	26.9 (3910)	0.15	13.8 (2.0)
-0149-2	1475	> 19.9 (> 2890)†	----	----
-0151-2	1485	21.8 (3160)	0.25	11.6 (1.6)
-0148-1	1980	> 21.9 (> 3180)†	> 0.55†	4.5 (0.65)
-0149-3	1950	> 20.7 (> 3010)†	> 0.33†	6.2 (0.90)
-0148-2	2400	5.2 (753)	0.90	2.1 (0.30)
-0151-1	2400	10.5 (1527)	1.50	1.4 (0.20)

†Broke in grip

Discussion

Based on the mechanical and thermophysical property results presented here and in preceding reports, it is obvious that the low (U,Zr)C content material (for a given processing -- e.g., extrusion) should be superior in a thermal stress environment. It has lower modulus, lower thermal expansion, higher thermal diffusivity, and a fracture strength which is not much lower than the higher carbide content material. We do not yet have data for varying carbide content for hot pressed material but this will come from Lot No. SL021.

In the next reporting period, the testing of Lot SL021 will be performed, and two new lots of fuel which are being produced at LASL will be characterized. These two new lots of fuel represent the best formulation of a graphite-matrix upgraded core fuel -- one made by hot pressing and the other by extrusion. The total uranium loading is 800 mg/cc with an enrichment of 62 percent. The uranium loading being produced is thought to be the level to be used in an actual production fuel to insure that the chemistry and processing are well established. The 62 percent enrichment was chosen to limit the peak surface temperature to 2500^{o}C in a full pulse ACPR pellet test.

CHAPTER VIII

Task 8. Driver Core Fuel Element
J. A. Reuscher, 5424

Introduction

The outer region of the Upgraded ACPR will consist of uranium-zirconium hydride fuel elements similar to the elements in the present ACPR core. This task is responsible for the in-pile testing and design of the U-ZrH elements.

In-Pile Tests

The specimens of uranium-zirconium hydride for the in-pile tests were received from General Atomic, San Diego. The H to Zr ratio varied from 1.46 to 1.59 and the length of the 3.56 cm diameter pellets varied from 0.32 to 12.7 cm All of the test apparatus is complete and the actual testing of these specimens will begin early in the next quarter.

CHAPTER IX

Task 9. Diagnostic System

Activities on this task for this reporting period are described in the Fast Reactor Safety Research Program - Quarterly Report, July-September 1976, SAND76-0652, Reactor Research and Development Department, Sandia Laboratories, Albuquerque, New Mexico, December 1976.

REFERENCES

1. Experimental Fast Reactor Safety Research Program - (Combined) Quarterly Report, July-December 1974, SAND75-0068, Simulation Sciences Research Department, Sandia Laboratories, Albuquerque, New Mexico, February 1975.

2. Experimental Fast Reactor Safety Research Program - Quarterly Report, January-March 1975, SAND75-0225, Simulation Sciences Research Department, Sandia Laboratories, Albuquerque, New Mexico, April 1975.

3. Experimental Fast Reactor Safety Research Program - Quarterly Report, April-June 1975, SAND75-0449, Reactor Applications Research Department, Sandia Laboratories, Albuquerque, New Mexico, August 1975.

4. Annular Core Pulse Reactor Upgrade - Quarterly Report, July-September 1975, SAND75-0630, Reactor Research and Development Department, Sandia Laboratories, Albuquerque, New Mexico, January 1976.

5. Annular Core Pulse Reactor Upgrade Quarterly Report, October-December 1975, SAND76-0165, Reactor Research and Development Department, Sandia Laboratories, Albuquerque, New Mexico, April 1976.

6. Annular Core Pulse Reactor Upgrade Quarterly Report, January-March 1976, SAND76-0281, Reactor Research and Development Department, Sandia Laboratories, Albuquerque, New Mexico, July 1976.

7. Fast Reactor Safety Research Program - Quarterly Report, July-September 1976, SAND76-0652, Reactor Research and Development Department, Sandia Laboratories, Albuquerque, New Mexico, December 1976.

8. J. F. Peterson, TAC-2D--A General Purpose Two-Dimensional Heat Transfer Computer Code, GA-8868, General Atomics, 1969.

9. L. Bernath, "A Theory of Local Boiling Burnout and Its Applications to Existing Date," Chem. Engr. Prog. Symp. Ser., Vol. 56, No. 30 (1960), p. 95.

DISTRIBUTION:

TID-4500 - NRC-7 (259)

Division of Reactor Safety Research (2)
U.S. Nuclear Regulatory Commission
Washington, DC 20555
Attn: W. S. Farmer, Research Applications Branch
J. C. Stone, Special Projects Branch

Division of Reactor Safety Research (7)
Office of Nuclear Regulatory Research
U.S. Nuclear Regulatory Commission
Mail Station: G-158
Washington, DC 20555
Attn: M. Silberberg, Chief, Experimental Fast Reactor Safety Branch (1)
R. W. Wright, Experimental Fast Reactor Safety Branch (6)

USERDA
Reactor Safety Branch
Division of Safety Standards and Compliance
Washington, DC 20545
Attn: M. A. Bell

USERDA
Division of Military Application (2)
Office of Safety and Facilities
Washington, DC 20545
Attn: R. T. A. Bredderman
H. M. Busey

USERDA
Division of Military Application
Program Analysis and Budget
Washington, DC 20545
Attn: L. M. Groover

Reactor Safety Research Coordination (4)
USERDA
Washington, DC 20545
Attn: R. W. Barber, Acting Director (3)
T. E. McSpadden, Project Manager (1)

USERDA
Division of Reactor Development and Demonstration
Washington, DC 20545
Attn: Assistant Director, Reactor Safety (Vacant)

USERDA
Division of Facilities and Construction Management
Washington, DC 20545
Attn: B. G. Edgerton

USERDA (2)
Operational Safety Division
Albuquerque Operations Office
P. O. Box 5400
Albuquerque, NM 87115
Attn: J. R. Roeder, Director
K. E. Elliott

Distribution (cont'd)

USERDA
Special Programs Division
Albuquerque Operations Office
P. O. Box 5400
Albuquerque, NM 87115
Attn: C. B. Quinn

USERDA
Engineering and Construction Division (2)
Albuquerque Operations Office
P. O. Box 5400
Albuquerque, NM 87115
Attn: M. E. Autio
A. R. Sneddon

Argonne National Laboratory (3)
9700 South Cass Avenue
Argonne, IL 60439
Attn: R. Avery
R. G. Matlock
D. Rardin

Lawrence Livermore Laboratory
Inorganic Materials Division
P. O. Box 808
Livermore, CA 94550
Attn: J. B. Holt

Los Alamos Scientific Laboratory (7)
P. O. Box 1663
Los Alamos, NM 87544
Attn: K. V. Davidson, CMB-6
W. G. Davey, A-DO
R. E. Peterson, DIR-FMO
T. F. Wimett, A-5
J. D. Orndoff, A-5
V. Starkovich, WX-6
W. E. Stein, P-DOR

University of California
Energy and Kinetics Department
5530 Boelter Hall
Attn: W. E. Kastenberg

Brookhaven National Laboratory
Fast Reactor Safety
Associated Universities, Inc.
Upton, Long Island, NY 11973
Attn: T. Ginsberg

University of Arizona
Department of Nuclear Engineering
Tucson, AZ 85721
Attn: R. Seale

General Electric Corporation (2)
310 De Guigne Drive
Sunnyvale, CA 94086
Attn: J. O. Bradfute
S. Kraus

General Atomic Company
TRIGA Division
P. O. Box 81608
San Diego, CA 92138
Attn: R. H. Peters

W. E. Nyer
P. O. Box 1845
Idaho Falls, ID 83401

Reactivity Accident Laboratory (2)
Division of Reactor Safety
Reactor Safety Research Center
Japan Atomic Energy Research Institute
Tokai-Mura, Ibaraki-Ken, Japan
Attn: Shinzo Saito
Michio Ishikawa

Electric Power Research Institute (3)
3412 Hillview Avenue
P. O. Box 10412
Palo Alto, CA 94304
Attn: M. Levenson
W. Loewenstein (2)

Dr. M. H. McTaggart
MOD(PE) Atomic Weapons Research
Establishment
Aldermaston
Berkshire, England

Mr. J. R. Findlay
Building 429
Atomic Energy Research Establishment
Harwell, Didcot
Berkshire, England

Dr. A. R. Baker
Fast Reactor Systems Directorate
UK Atomic Energy Agency
Warrington
Cheshire, England

2 W. J. Howard
1000 G. A. Fowler
1100 C. D. Broyles
1126 G. L. Ogle
1130 H. E. Viney
1136 J. H. Davis
1136A J. A. Brammer
1136A D. K. Overmier

Distribution (cont'd)

1200 W. A. Gardner
1280 T. B. Lane
1283 H. C. Hardee
1283 C. E. Sisson
1300 D. B. Shuster
3241 J. A. DeVargas
3284 A. W. Porter
3284 R. P. Tyler
3310 W. H. Kingsley
4010 C. Winter
5100 J. K. Galt
5110 F. L. Vook
5120 G. J. Simmons
5130 G. A. Samara
5160 W. Herrmann
5200 E. H. Beckner
5200 M. J. Becktell
5230 M. Cowan, Jr.
5232 L. D. Posey
5240 G. Yonas
5400 A. W. Snyder
5410 D. J. McCloskey
5420 J. V. Walker (10)
5420A H. D. Kubiak
5420A W. H. Myers
5421 T. R. Schmidt
5422 R. L. Coats
5422 D. J. Sasmor
5423 J. E. Powell
5423 G. A. Carlson
5423 L. M. Choate
5423 L. R. Edwards
5423 J. G. Kelly
5423 H. L. Scott
5423 W. H. Sullivan
5423 S. A. Wright
5424 J. A. Reuscher (10)
5424 F. M. Morris
5424 P. S. Pickard
5430 R. M. Jefferson
5440 R. W. Lynch
5700 J. H. Scott
5800 R. S. Claassen
5820 R. L. Schwoebel
5830 M. J. Davis
5840 H. J. Saxton
5846 E. K. Beauchamp
5846 R. H. Marion
5847 C. H. Karnes
8300 B. F. Murphey
8310 D. M. Schuster
9512 W. P. Thomas
9700 R. E. Hopper
9750 R. W. Hunnicutt
9750 F. J. Tuffs
8266 E. A. Aas (2)
3141 C. A. Pepmueller, Actg. (5)
3151 W. L. Garner (3)
For ERDA/TIC (Unlimited Release)

☆ U S GOVERNMENT PRINTING OFFICE 1977—777-019/502